

The Lactocrine Hypothesis and Laser Microdissection: Evaluating Tissue-Specific Effects of Milk-Borne Factors on Gene Expression in the Neonatal Porcine Uterus

by

Dori Jill Miller

A thesis submitted to the Graduate Faculty of
Auburn University
in partial fulfillment of the
requirements for the Degree of
Master of Science

Auburn, Alabama
August 2, 2014

Keywords: uterine development, lactocrine, ESR1, pig, laser microdissection

Copyright 2014 by Dori Jill Miller

Approved by

Frank F. Bartol, Chair, Alumni Professor of Anatomy, Physiology and Pharmacology
Jacek Wower, Professor of Animal Science
Richard C. Bird, Professor of Pathobiology
Terry D. Brandebourg, Assistant Professor of Animal Science

Abstract

In the pig, development of the uterus begins *in utero* and is promoted postnatally via communication of milk-borne bioactive factors (MbFs) that advance development of neonatal somatic tissues. The passage of MbFs from mother to neonate is termed lactocrine signaling. The porcine endometrium is estrogen receptor (ESR1) –negative and relaxin (RLX) receptor (RXFP1) –positive at birth (postnatal day 0 = PND 0). Expression of stromal ESR1 by PND 2 is directly associated with the onset of uterine gland genesis. Data for RLX in milk suggests that a critical lactocrine programming window for uterine development exists between birth and PND 2. Developmental disruption between PND 0 and 14 reduces uterine capacity in the adult. The extent to which lactocrine signaling affects organizationally critical stromal-epithelial interactions and resulting morphological changes is unknown. Laser microdissection (LMD) is a tool that can be used to physically separate specific cell or tissue types from histological preparations for use in molecular analysis. However, application of LMD for such purposes presents technical challenges and optimization of these factors is necessary to obtain robust data. Here, objectives are to i) review aspects of uterine development, ii) establish a protocol for the use of LMD in evaluating stromal-epithelial interactions that drive uterine development and iii) determine the effects of nursing for 48 h from birth on

endometrial compartment-specific ESR1, RXFP1, vascular endothelial growth factor (VEFGA) expression and uterine morphology as seen on PND 2 and PND 14.

Acknowledgments

I would first like to thank my mentor, Dr. Frank (Skip) Bartol for all of his insight, guidance and support of my endeavors. I also extend my sincere gratitude to Ms. Anne Wiley for her incomparable lab skills and for keeping me sane when nothing seemed to work. To my lab mates (at both Auburn and Rutgers), Bethany Crean-Harris, Dr. Amy Campbell, Alejandro Silva, Elizabeth Talley, Meghan Davolt, Dr. Joseph Chen, and Dr. Amy Frankshun, it was a pleasure being in the trenches with you.

Without the invaluable assistance of Mr. Brian Anderson and the members of the AU/RU pLac /AU-CVM BRaTs undergraduate research team none of this would have been possible. Thank you for giving up your time to whisper to pigs and to spend countless sleepless nights with me.

Last, but most definitely not least, thank you to my family and friends for all of your encouragement, support, and patience.

Table of Contents

Abstract.....	ii
Acknowledgments.....	iv
List of Tables	viii
List of Figures	ix
List of Abbreviations	x
Introduction.....	1
Chapter 1: Literature Review	4
1.1 The Pig	4
1.2 The Uterus	4
1.3 Uterine Morphology	5
1.4 Uterine Histology	6
1.5 Postnatal Development	6
1.5.1 Gland Genesis	7
1.6 Mechanisms of Gland Development	7
1.6.1 Stromal-Epithelial Interactions	8
1.6.2 Estrogen Receptor and Gland Genesis	9
1.6.3 Morphoregulatory Genes and Gland Genesis	10
1.6.4 Relaxin Receptor and Gland Genesis	11
1.6.5 VEGFA and Gland Genesis	12

1.7 Uterine Functions	13
1.7.1 Maternal Recognition of Pregnancy	13
1.7.2 Uterine Capacity	14
1.8 Developmental Programming	14
1.9 Lactocrine Programming	16
1.9.1 Milk as a Conduit for Developmental Signals	16
1.9.2 RLX as the prototypical MbF	17
1.9.3 Lactocrine Programming of the Porcine Uterus	18
1.10 Laser Microdissection	20
1.11 Principles	21
1.12 Applications	21
1.13 Limitations	22
1.13.1 Fixation	22
1.13.2 Tissue Processing	25
1.13.3 Procedural Adaptations	25
1.14 Summary and Implications	26
Chapter 2: Laser Microdissection as a Tool to Evaluate Endometrial Cell-Compartment Specific Gene Expression in Fixed Tissues	28
2.1 Abstract	28
2.2 Introduction	29
2.3 Materials and Methods	31
2.4 Results	33
2.5 Discussion	34

Chapter 3: Nursing for 48 h from Birth Supports Porcine Uterine Gland Development and Endometrial Cell-Compartment Specific Gene Expression	42
3.1 Abstract	42
3.2 Introduction	43
3.3 Materials and Methods	46
3.4 Results	50
3.5 Discussion	52
References.....	68
Appendix A: Laser Microdissection Slide Preparation	96
Appendix B: Laser Microdissection Process	98
Appendix C: LMD of Uterine Tissues	101
Appendix D: RNA Extraction.....	102
Appendix E: Quantitative Real Time-PCR	105
Appendix F: Immunohistochemistry	108

List of Tables

Table 1. Target porcine ESR1, RXFP1, and S15 accession numbers, forward and reverse primers and amplicon size	37
Table 2. Targeted porcine gene accession numbers, forward and reverse primer sequences and predicted amplicon size	61

List of Figures

Figure 1. Laser microdissection (LMD) of neonatal porcine endometrial stroma and epithelium	37
Figure 2. Validation of qPCR results in PND 2 endometrial samples	38
Figure 3. Validation of qPCR results in PND 14 endometrial samples.....	39
Figure 4. Cell-compartment specific ESR1 mRNA expression on PND 2 and PND 14.....	40
Figure 5. Cell-compartment specific RXFP1 mRNA expression on PND 2 and PND 14	41
Figure 6. Experimental design	62
Figure 7. Endometrial histoarchitecture affected by age and nursing	63
Figure 8. Endometrial PCNA immunostaining and labeling indices affected by neonatal age and nursing	64
Figure 9. Endometrial ESR1 immunostaining and labeling indices affected by neonatal age and nursing	65
Figure 10. Endometrial tissue compartment-specific expression of ESR1 (A), VEGFA (B) and RXFP1(C) mRNA on PND 2 (left) and PND 14 (right) in gilts nursed (open bars) or fed milk replacer (closed bars) for two days from birth	67

List of Abbreviations

bp	base pairs
<i>E</i>	standard curve efficiencies
ESR1	estrogen receptor
EV	estradiol valerate
GE	glandular epithelium
GI	gastrointestinal tract
LCM	laser capture microdissection
LE	luminal epithelium
LI	labeling index
LMD	laser capture microdissection
LSM	least squared means
MbF	milk-borne bioactive factor
miRNA	micro RNA
MIS	Müllerian Inhibiting Substance
MMP	matrix metalloproteinases
Myo	myometrium
NBF	neutral buffered formalin
OCT	Optimum Cutting Temperature medium
PCNA	proliferating cell nuclear antigen

PGF2 α	prostaglandin F2 α
PND	postnatal day
PR	progesterone receptor
qPCR	quantitative real-time polymerase chain reaction
RLX	relaxin
ROI	region of interest
RXFP1	relaxin receptor
SEM	standard error
St	stroma
S15	ribosomal protein
VEGF	vascular endothelial growth factor

Introduction

Reproductive success of an adult female mammal is dependent upon many things including interplay of environmental, nutritional and biological factors. Proper development of the female reproductive tract is required to insure an adult animal's ability to successfully reproduce. The female reproductive tract is composed of the oviducts, uterus, cervix, and vagina [1]. This review will focus on the development of the porcine uterus. The uterus is an essential reproductive organ. Uterine functions include: sperm transport, recognition of pregnancy, maintenance of an embryotrophic environment, and expulsion of the fetus at the time of parturition [1]. For the uterus to be able to perform these functions it must undergo a series of critical morphological changes from conception to adulthood. This involves complicated interactions between genes, cell types, hormones, growth factors, and receptors [2, 3].

In the pig, *Sus scrofa domesticus*, development of the uterus begins in utero and continues postnatally [4]. At birth (postnatal day = PND 0), the immature uterus lacks uterine glands [5]. Proper gland formation is brought about by structural changes in the myometrium (Myo), luminal epithelial (LE), glandular epithelium (GE) and stroma (St). This process involves differentiation of GE from LE and formation of coiled glands that penetrate into underlying stroma [6]. Expression of stromal estrogen receptor (ESR1) occurs by PND 2 and estrogen activity drives the temporospatial expression of other uterine morphoregulatory genes that aid endometrial tissue remodeling [5, 7, 8]. Data for the pig show that disruption of

ESR1 expression and activation within the first 14 days of life alters the uterine developmental program and hinders reproductive success of the adult [2, 9, 10]. Bioactive relaxin (RLX) is found in the milk of lactating sows for 48 h following parturition and can subsequently be found in the circulation of nursing pigs for 48 h following birth [11-13]. Unlike ESR1, the RLX receptor (RXFP1) is present in endometrial stroma at birth [13]. Collectively, these data led to the development of the feed-forward mechanism for the RXFP1-mediated, estrogen-sensitive, gene expression events in the neonatal porcine endometrium [4]. The lactocrine hypothesis states that milk-borne bioactive factors (MbFs), such as RLX, are passed from mother to offspring as a consequence of nursing and these factors act in the neonate to support normal somatic tissue development [4, 11]. Lactocrine delivery of hormones and growth factors may help to establish and maintain the developmental program of the uterus as well as other tissues/organs [14-16].

Cross-talk between ESR1 and RXFP1 may regulate the temporospatial expression of morphoregulatory genes and thereby facilitate stromal-epithelial interactions that result in differentiation, proliferation, and organization of cell populations to form uterine glands. Laser microdissection (LMD) is a tool that can be used to better understand changes occurring within isolated cell populations. Using LMD, single cells or entire cell populations can be excised and isolated for use in downstream molecular analyses such as quantitative PCR (qPCR) [17, 18]. Due to the delicate nature of target molecules like RNA, laser microdissection involves optimization throughout the process and encompasses everything from fixation to

analytical procedures [19-21]. This technique is ideal to evaluate the effects of lactocrine signaling on endometrial cell-compartment specific gene expression.

Chapter 1:

Literature Review

1.1 The Pig

The pig, *Sus scrofa domesticus*, is both an important laboratory and agricultural animal [22-29]. The female pig is a non-seasonal breeder with reoccurring estrous cycles of 21 days in length and are spontaneous ovulators [1]. Estrus duration can range from 2-4 days [1, 30]. Pigs are a litter-bearing, or polytocus, species that typically have litter sizes of 10-12 piglets [30]. Gilts reach sexual maturity at 6-8 months of age at which time the uterus is capable of supporting and maintaining pregnancy [1]. Over the course of the animal's life, the uterus undergoes a series of developmental changes that allow pregnancy to occur. Development and characteristics of the porcine uterus are discussed below.

1.2 The Uterus

The female reproductive tract includes the oviducts, uterus, cervix, and vagina. Development of the female reproductive tract begins prenatally in the absence of a Y chromosome and Müllerian inhibiting substance (MIS). In males, MIS causes the regression of the Müllerian ducts from which the female reproductive tract is derived. The absence of MIS allows for the formation of the ovaries and the development of the female phenotype [31]. The embryonic origins of the Müllerian ducts have been characterized in mice [31, 32]. Specialized cells from the coelomic epithelium begin

to invaginate caudally to form the Müllerian ducts. The ducts then elongate caudally toward the urogenital sinus. Upon reaching the urogenital sinus the two ducts begin to fuse, forming a single tubular organ. The posterior fused portion becomes the vagina, cervix, and uterine body while the anterior un-fused portion becomes the uterine horns and oviducts [3, 32]. The degree of fusion varies between species and determines the specific uterine classification. Fusion can be described as complete, partial, or incomplete. Uterine types include i) simplex; found in humans and primates, ii) bicornuate; found in pigs, sheep and cattle and iii) duplex; found in marsupials [1].

1.3 Uterine Morphology

The uterus is a tubular, muscular organ located in the pelvis between the bladder and rectum. The sow has a bicornuate uterus formed from partial fusion of the two Müllerian ducts. The uterine horns, or cornua, are approximately 150-200 cm in length and come together to form the uterine body which is approximately 5 cm in length [30]. The uterine body and horns are luminal structures lined by the mucosa or endometrium. The endometrium is surrounded by muscularis or myometrium. The sersosa or perimetrium forms the outer covering of the uterus. The uterus is supported in the body cavity by the portion of the broad ligament called the mesometrium [1, 3].

1.4 Uterine Histology

In the pig, radial patterning of the uterus begins prenatally and is completed postnatally [3, 33]. Radial patterning allows for differentiation of the three main layers of the uterine wall: the endometrium, myometrium and perimetrium. The endometrium is derived from Müllerian mesenchymal cells and consists of three major cell types: luminal epithelium, glandular epithelium, and stroma. Both GE and LE are composed of simple cuboidal cells [2, 34, 35]. The subluminal region of the endometrium consists of a dense layer of stratified stromal cells and a loose network of fibroblasts [2]. Uterine stroma is divided into 3 regions: i) stratum compactum which is adjacent to the LE, ii) stratum spongiosum is the middle layer that surrounds the uterine glands, and iii) stratum basalis that lies adjacent to the myometrium [6]. The myometrium is composed of an inner circular layer and outer longitudinal layer of muscle. The perimetrium is a thin layer of serosal tissue derived from embryonic mesoderm and forms the outer protective layer of the uterus [1].

1.5 Postnatal Uterine Development

Endometrial glands are the functional unit of the endometrium and secrete a cocktail of proteins, referred to as uterine milk [36] or histotroph, that supports conceptus implantation, growth, and survival [37, 38]. In many species, including pigs [39], rats and mice [40], and sheep [41], the uterus is devoid of glands at birth. Proper development of endometrial glands occurs between birth and adulthood through a series of molecular and morphological changes. If endometrial glands fail

to form properly it can result in the inability of the uterus to respond to conceptus signals compromise the reproductive health of the adult [9].

1.5.1 Gland Genesis

Adenogenesis, or gland development, in the neonatal porcine uterus involves a series of both histological and molecular changes from birth until adulthood. At birth, the LE of the endometrium is relatively smooth with only shallow and infrequent depressions that mark the beginnings of what will become a complex network of tubular, coiled and branched uterine glands. By PND 3, LE begins to invaginate and nascent GE can be observed [42]. Simple glands are seen by PND 7 in shallow stroma and by PND 14 tubular, coiled glands penetrate deeper into the stroma [43]. By PND 28, coiled glands extend to the myometrium and uterine folds are apparent [43]. The endometrium on PND 56 contains coiled, branched glands and more prominent uterine folds [43]. By PND 120, the uterine wall reaches functional maturity and, therefore, is capable of responding to conceptus signals and supporting pregnancy [2, 44].

1.6 Mechanisms of Gland Development

As noted above, in the first few weeks of life the porcine endometrium undergoes a series of morphological changes driven by underlying molecular, cellular, and hormonal events [6]. Differentiation and proliferation of GE is dependent on microenvironmental factors that may be the result of stromal-epithelial interactions or cellular responses to hormones like estrogen and relaxin. Although

mechanisms such as these are slowly becoming more clear there is still much to be investigated and understood.

1.6.1 Stromal-Epithelial Interactions

Coordination of morphological changes leading to the functional maturation of the uterus is dependent upon stromal-epithelial interactions [3, 45]. How these two cellular compartments communicate with one another is based on the idea that factors (hormones, growth factors, cytokines) expressed by the stroma act in the epithelium, and vice-versa, to promote epithelial proliferation and differentiation resulting in the formation of uterine glands [2, 9]. Stromal influence has been demonstrated in tissue recombination studies using perinatal mice. Vaginal stroma induced uterine epithelium to take on characteristics of vaginal epithelium. Likewise, uterine stroma induced the transformation of vaginal epithelium to uterine epithelium [34, 46]. This study also revealed that stromal-epithelial effects occur in a time dependent manner such that cytodifferentiation of both vaginal and uterine epithelium had occurred by PND 10 suggesting a critical developmental window [46]. Interestingly, an *in vivo* study using rat tissues showed that in the absence of uterine epithelial cells, uterine stromal cells do not decidualize following hormonal stimulus [47, 48]. In another murine tissue recombination study, vaginal epithelium did not induce uterine stromal proliferation in response to hormonal stimulation; however uterine epithelium did induce proliferation in uterine stroma [7]. Together these studies illustrate stromal-epithelial communication is necessary to promote cytodifferentiation and proliferation and that signals between cell types are organ specific. Data for the pig and sheep, like

data for mice and rats, indicate gland genesis is mediated by local factors that induce epithelial cell differentiation [8, 43], however, stromal-epithelial interactions may target the basal lamina allowing for migration of GE into the stroma rather than be dependent on epithelial proliferation [45]. Together these data indicate that stromal and epithelial signals act in a cell compartment and organ-specific manner to allow for the differentiation and reorganization of the endometrium. The identity of all factors mediating stromal-epithelial interactions is unknown. Some key players include hormones, cytokines, morphoregulatory genes, growth factors, and matrix metalloproteinases (MMPs) [3, 6].

1.6.2 Estrogen Receptor and Gland Genesis

The steroid hormone estrogen is a known catalyst of epithelial differentiation. The estrogen receptor was first isolated from rat uterine tissue in the 1960s [49, 50]. The estrogen receptor is a nuclear receptor with the primary function of regulating gene transcription [51, 52]. However, there are G-coupled membrane-associated receptors linked to estrogen signaling as well [53]. Two forms of the estrogen receptor, ESR1 and ESR2 (formerly referred to as ER α and ER β), are found in the uterus with ESR1 being the predominant form [54-56]. At birth, murine uterine epithelium is ESR1-negative while uterine stroma is ESR1-positive [57]. Interestingly, estradiol exposure induced cell proliferation in ESR1-negative uterine epithelium [58, 59]. Similarly, ESR1 expression in the neonatal pig is absent at birth, but is localized to the stroma and nascent GE by PND 2 [5, 60]. Similar to the mouse, neonatal estrogen exposure advanced gland genesis in ESR1-negative

epithelial cells. Expression of proliferating cell nuclear antigen (PCNA), a maker of cell proliferation, mirrors that of ESR1 in the porcine endometrium [42]. Thus, estrogen is a uterotrophic hormone as denoted by ESR1-positive stromal cells supporting, through cell interactions, the proliferation of ESR1-negative uterine epithelium [61].

1.6.3 Morphoregulatory Genes and Gland Genesis

Morphoregulatory genes, and their products, in the Wnt and Hoxa families play an important role in the regulation of endometrial differentiation and development via the mediation of stromal-epithelial interactions and cell proliferation. Members of these families commonly associated with adenogenesis include: *Wnt4*, *Wnt5a*, *Wnt7a*, *Hoxa10*, and *Hoxa11*. These genes follow distinct cell-compartment expression patterns in the endometrium. In the neonatal mouse, *Wnt7a* is localized to LE while *Wnt4*, *Wnt5a*, *Hoxa10*, and *Hoxa11* are found in stroma [62-66]. The expression patterns of these genes in the mouse are similar to that of neonatal pig [33]. Studies in the mouse have begun to shed light on the importance of the individual functions and interactions of these genes. The uterus of mice lacking *Wnt5a* and *Wnt7a* expression (either in combination or individually) in female reproductive tract tissues are aglandular suggesting both genes are required for gland formation [67]. *Hoxa10* and *Hoxa11* mutant mice also show altered uterine morphology [65, 67]. In *Wnt4* knockout mice, there is a complete absence of Müllerian ducts [68]. Another important morphoregulatory gene is *Msx2*. This gene was determined to be a regulator of both *Wnt7a* and *Wnt5a* expression [69]. All of

these genes work together under hormonal stimulus in a controlled loop, known as the WNT/HOXA axis, to create a permissive environment for adenogenesis.

Under estrogen stimulation, epithelial *Wnt7a* regulates stromal expression of *Wnt4* and *Wnt5a* which in turn regulate stromal expression of *Hoxa10* and *Hoxa11*. *Msx2* acts to balance out the system by regulating *Wnt5a* and *Wnt7a*. Activity of this feedback loop permits differentiation of GE from LE and reorganization of the stroma to allow gland penetration. In the pig, estrogen exposure from birth, downregulated *Wnt4*, *Wnt5a*, and *Wnt7a* expression while upregulating *Hoxa10* expression [33]. Neonatal estrogen exposure also resulted in increased glandularity as seen on PND 14 [70] and reduced litter sizes [2] showing that prematurely advancing gland genesis, via estrogen exposure, results in subfertile adults. Collectively, these data provide evidence for the mechanism of estrogen regulation of the WNT/HOXA axis and subsequent gland genesis.

1.6.4 Relaxin Receptor and Gland Genesis

Relaxin is a 6 kDa peptide hormone that was first discovered by Frederick Hisaw [71] as the substance responsible for relaxing the interpubic ligament of guinea pigs and, therefore, is traditionally considered a reproductive hormone that targets connective tissue. Since then, RLX has been found to have a wide range of biological functions which include being a uterotrophic hormone [5, 72]. The RLX receptor, RXFP1, is a leucine-rich repeat containing, G-coupled protein receptor [73]. RXFP1 is primarily localized to endometrial stroma in rodents [74, 75] as well as the pig [13]. In one study involving mice, RXFP1 was localized to stromal cells and administration

of exogenous RLX stimulated epithelial cell proliferation in the cervix and vagina [61]. A follow-up to this study using ESR1 knock-out mice determined that the proliferative response to RLX, in both cervical stroma and epithelium, is dependent on stromal ESR1 expression [76]. Likewise, neonatal pigs treated with RLX had increased uterine expression of ESR1 [60]. Together, these studies support not only the idea for the necessity of stromal-epithelial interactions, but that cross-talk between RLX and estrogen signaling systems drive endometrial development.

1.6.5 VEGF and Uterine Development

As organs grow and develop so must the vascular networks that support them. Vascular endothelial growth factor (VEGFA) stimulates angiogenesis, or the growth of new blood vessels, eliciting anti-apoptotic cellular responses on target endothelial cells [77, 78]. So, it follows that VEGFA regulates the vascularization of proliferating tissues. In fact, VEGFA has been found in the endometrium of primates, rodents, and pigs [79-81]. In studies involving primates [81], rats [82, 83], humans [84], and pigs [60] estrogen exposure resulted in increased VEGFA expression in uterine tissues. In the study [60] involving neonatal gilts, animals were exposed to either estrogen or relaxin and both treatments resulted in the upregulation of VEGFA. Therefore, expression of VEGFA is both estrogen and relaxin sensitive in the neonatal pig. Once again this supports the idea that estrogen and relaxin work together to promote uterine development.

1.7 Uterine Functions

As previously stated, normal development of the uterus is crucial to ensure reproductive success of the adult. Reproductive success is determined by the ability of the uterus to carry out primary functions which include: sperm transport, recognition of pregnancy, maintenance of an embryotrophic environment, and expulsion of the fetus at the time of parturition [1]. Here, the ability of the uterus to establish then maintain pregnancy (i.e. uterine capacity) will be discussed.

1.7.1 Maternal Recognition of Pregnancy

Conceptus implantation is dependent on ability of the uterus to respond to conceptus signals and allow establishment of the maternal-conceptus interface. In the pig, estrogen secreted by the conceptus on gestation day 12 is responsible for maternal recognition of pregnancy [85]. Maternal recognition of pregnancy is the process by which the conceptus signals the mother so that luteal sources of progesterone can be maintained and pregnancy can be established [86]. If the uterus is receptive, estrogen will almost immediately induce the exocrine, rather than endocrine, secretion of prostaglandin $F2\alpha$ ($PGF2\alpha$) preventing luteolysis [79, 86, 87]. Progesterone from the corpora lutea is essential for the transformation of the endometrium into an embryotrophic environment. Progesterone receptors (PR) are localized to LE, GE, and stroma but by pregnancy day 12 PR is predominantly found in GE [88]. Thus, progesterone acting on GE receptors results in the secretion of embryotrophic proteins and allows for successful implantation [86, 89].

1.7.2 Uterine Capacity

Establishment of pregnancy does not guarantee embryo survival. Uterine capacity is defined as the number of embryos the uterus is able to maintain at a given time point in gestation as related to the surface area of placental-endometrial attachment [90, 91]. Although all determinants of uterine capacity are unknown, disruption of neonatal uterine development is a known cause of embryo losses. In the pig, the majority of embryo loss occurs before pregnancy day 25 [92]. It is established that exposure to estradiol valerate (EV) for two weeks from birth alters neonatal porcine uterine histoarchitecture [8]. One study investigated whether or not EV exposure for two weeks from birth would affect uterine capacity [2]. Gilts were bred following their second estrus and conceptus numbers were evaluated on pregnancy day 45. Neonatal estrogen exposure resulted in reduced litter sizes in comparison to control animals suggesting that disruption of normal developmental events reduces uterine capacity of the adult [2]. A later study, [93] using the same protocol, found that neonatal exposure to EV altered the normal uterine gene expression profile. Together these data show that alterations in the neonatal uterine developmental program can affect uterine histoarchitecture such that recognition, establishment, and maintenance of pregnancy are disrupted [33].

1.8 Developmental Programming

Developmental programming was defined by Nijland et al. [94] as “*the response by developing mammalian organisms to a specific stimulus or insult during a critical time window that alters the trajectory of development with resulting*

persistent effects on phenotype.” Basic principles associated with this concept include the following: i) critical developmental periods exist during which an organism will be more vulnerable to insults or stimuli; ii) programming involves morphological changes in tissues and organs; iii) insults and stimuli can have permanent effects on the organism; and iv) these effects can be transgenerational [95]. Critical periods of development can be defined as times during which cell number is rapidly increasing and essential organizational and physiological changes are taking place [94, 95]. Because all species do not follow the same growth patterns, critical developmental periods vary between species, as well as organs and tissues [94-96].

Epigenetic mechanisms control developmental programming events. Consequently, epigenetic processes are defined by alterations in phenotype that occur without alteration to the genome [97, 98]. Central mechanisms of epigenetics include DNA methylation, chromatin packaging, and microRNA (miRNA) stabilization, all of which can result in gene silencing [99]. Such modifications in the fetus or neonate can be permanent and/or transgenerational [98]. Pre- and postnatal changes in developmental programming can have detrimental repercussions in adulthood. Maternal programming can be defined as maternal factors that affect both pre- and postnatal development of offspring [100]. Factors such as maternal and neonatal nutrition and exposure to environmental endocrine disruptors can affect disease susceptibility, behavior, organ development, and reproductive performance [4, 33, 101-104].

Programming of the porcine uterus is established at conception and continues postnatally as discussed above [4]. The sequence of molecular and morphological events associated with neonatal uterine development follow a developmental trajectory that determine the function of the cells within the uterus [105]. Therefore, altering developmental trajectory can ultimately alter uterine phenotype. Maternal programming of the porcine uterus, as for all nursing mammals, does not end at birth. The mother maintains influence, though diminished in comparison to the influence *in utero*, after birth through communication bioactive factors in milk [4, 13, 33]

1.9 Lactocrine Programming

The idea that all mammals nurse is not novel and the nutritional and immunological value of nursing to newborn mammals is well documented [106-108]. However, the impact of nursing on establishing the developmental program of neonates is an emerging story. Throughout the development of an organism there exist critical developmental windows or periods in which an animal may be more sensitive to disruptions in the program [100]. Lactation has shown to be one of these critical periods.

1.9.1 Milk as a Conduit for Developmental Signals

Colostrum, or first milk, is rich in fats, carbohydrates, proteins, and immunological factors that support neonatal growth and health [107, 109, 110]. Colostrum and mature milk also carry an array of bioactive peptides, growth factors, and steroid hormones [14, 111-114]. Studies have shown that milk-borne bioactive

factors (MbFs) consumed by neonates are absorbed in the gastrointestinal tract and promote the proliferation, differentiation, and growth of neonatal somatic cells, tissues, and organs [115-119]. Thus, colostrum acts as a conduit for maternal MbFs. The passage of these factors from mother to offspring as a consequence of nursing is known as lactocrine signaling [4]. The full extent to which lactocrine-active factors promote neonatal growth is unknown; however, data to be presented below support the concept of lactocrine programming of neonatal development.

1.9.2 RLX as the Prototypical MbF

RLX is found in the milk of several species including rats [120], dogs [121, 122], humans [123], and pigs [13]. Given that exogenous RLX induced uterotrophic effects on the porcine endometrium when given from birth [5], studies were conducted to determine if endogenous, milk-borne RLX had similar effects. First, it was determined that immunoreactive RLX was present in the highest concentrations for the first two days of lactation and was only detectable for two days of life, coinciding with gut closure, in piglets that nursed their mothers [13]. Thus, colostrum is the primary source of RLX in newborn pigs and the first two days of life mark the critical window for lactocrine delivery of MbFs. It was also established that the bioactive form of RLX in milk was the 18 kDa proRLX [12, 124]. Interestingly, bioactive peptides in milk can be encrypted within larger peptides (i.e. RLX within proRLX) that may be cleaved via proteolysis in the digestive tract [125, 126]. In fact analysis of porcine colostrum revealed, based on cleavage sites and peptide size, there could potentially be thousands of bioactive peptides in milk [125]. It has yet to be

determined whether or not proRLX or RLX is responsible for RLX-associated development of the uterus.

Development of the porcine endometrium is both ESR1-dependent and estrogen-sensitive [2, 70, 93]. At birth the porcine endometrium is ESR1-negative [5], but stromal cells are RXFP1-positive . By PND 2, ESR1 can be detected in the stroma and nascent GE [60]. The temporospatial expression of ESR1 coincides with the onset of gland development and disruption ERS1-associated developmental events within the first two weeks of life negatively affect the reproductive efficiency of the adult [2, 10]. Administration of estradiol-17 β upregulates the expression of RXFP1 by PND 2 [60]. Exogenous RLX exposure increased ESR1 and VEGFA expression by PND 2 [60] and had overall uterotrophic effects as seen on PND 14 [42]. Also, pretreatment of ICI 182,780, an estrogen receptor antagonist, attenuated the uterotrophic effects of RLX [42] indicating cross-talk between the two receptor systems may promote the expression of ESR1. Collectively, these data led to the development of feed-forward, lactocrine-driven mechanism for the development of the neonatal porcine uterus [4, 127].

1.9.3 Lactocrine Programming of the Porcine Uterus

In order to fully evaluate effects of lactocrine signaling on ESR1-dependent, estrogen-sensitive development of the neonatal porcine uterus studies were conducted in which neonatal gilts were fed a commercial-milk replacer or allowed to nurse their mother for 48 h from birth [128]. Effects of the lactocrine-null state (replacer-fed) were evaluated on both PND 2 and 14. By PND 2, protein expression of ESR1 was

undetectable in replacer-fed gilts, but present in nursed gilts [128]. The same effect was seen on VEGFA expression. To determine the extent to which milk-borne RLX effects ESR1 and VEGFA expression, exogenous RLX was administered to both replacer-fed and nursed animals. Exogenous RLX increased ESR1 and VEGFA protein expression in nursed gilts, but failed to recover the expression of either in replacer-fed gilts [128]. This suggests that RLX alone is not enough to support ESR1 expression. Evaluation of whole uterine ESR1 mRNA expression yielded similar results while VEGFA mRNA expression was increased by exogenous RLX, but not by imposition of the lactocrine-null state. RXFP1 mRNA expression was increased in response to the lactocrine-null state; however, exogenous RLX returned RXFP1 expression back to the level of nursed gilts. This indicates that RLX may regulate RXFP1 through a negative feedback mechanism. Expression levels of MMP9, which is important for tissue remodeling, were also decreased in replacer-fed animals at the level of the protein, but not mRNA expression. It is possible that the differences seen in VEGFA protein and mRNA expression is due to post-translational modification [128]. In a subsequent study, gilts either nursed or received replacer for 48 h from birth and then were allowed to continue nursing their mothers or were placed back on their mothers and allowed to nurse normally until PND 14. Protein expression of ESR1 and VEGFA was once again undetectable in the lactocrine-null gilts [129]. Similar data was also seen for ESR1 and VEGFA protein expression in the cervix on both PND 2 and PND 14 [130]. These results clearly show that factors in colostrum, including RLX, are required for establishment and maintenance of the uterine developmental program and that disruption of development during this lactocrine

programming window can offset the developmental trajectory as seen by molecular changes on PND 14. However, the extent to which these changes affect the uterine phenotype or reproductive success of the adult is unknown.

As previously discussed, the onset of gland genesis is dependent on the temporospatial expression patterns of ERS1 and RXFP1 in the neonatal porcine uterus. The stromal-epithelial interactions that fuel these changes are poorly understood. Being able to determine the effects of imposition of the lactocrine-null state on gene expression at the level of the cell compartment would provide new insight to how cell interactions promote uterine development.

1.10 Laser Microdissection

Understanding cellular interactions and the microenvironments in which they transpire is critical to decoding events that drive normal tissue development. Until recent years, evaluating isolated cell types within a tissue was difficult if not impossible. Microdissection of tissues was a crude, time consuming, manual process that only allowed for the dissection and analysis of large regions of tissues most likely containing many cell types [18, 131, 132]. Laser microdissection (LMD), or laser-capture microdissection (LCM), was developed at the National Cancer Institute with the purpose of evaluating tumor cell populations [18]. LMD is a tool that allows for the isolation of groups of cells or single cells from histological preparations or live cell culture [18, 133] and the use of those cells for molecular analysis of highly pure cell or tissue types [17].

1.11 Principles

The basic principles of LMD are that an investigator is able to i) visualize a region of interest (ROI) via microscope, ii) excise the ROI via the use of a laser, and iii) isolate the pure ROI from a tissue section or cell culture [133]. LMD can be performed on most tissues and cell types. Protocols for the extraction of RNA, DNA, and proteins from LMD derived cell populations are available for both frozen and fixed tissues. Current LMD systems allow the user to identify ROIs within tissue sections using a modified inverted microscope usually equipped with a motorized stage and camera that is able to display the image on a computer screen. Using computer based technology the investigator can designate the ROI to be excised and a software system then controls the firing and precision of the laser [134]. Once excised, the ROI can be isolated from the tissue section. The most common way of doing so uses micro-centrifuge tubes with caps that have adhesive coatings. The caps make contact with the tissue section or by using energy from the laser to transfer the ROI to a micro-centrifuge tube [17, 131, 132]. In some live cell culture preparations the laser is used to ablate one cell or cell type in order to isolate another. Isolation of these cells is still accomplished by using a micro-centrifuge tube.

1.12 Applications

The goal of LMD is to provide a means for the evaluation of the temporospatial characteristics of isolated tissues or cells and their microenvironments. Due to the increasing accessibility of this technique it has become a universal tool and has been employed in many life science fields. LMD-derived cell populations have

been used in applications involving genomic profiling [135], DNA methylation assays [136], 2 DE-gel electrophoresis [137-139], western blots [137], mass spectrophotometry [140, 141], immunohistochemical labeling [142, 143], *in situ* hybridization [144] and gene expression analysis [145-147]. This technique has been applied in the fields of plant biology [148, 149], forensic sciences [150], clinical sciences [151], genomic research [135, 148], pathology [152-154], cancer biology [17, 155], and developmental biology [145, 146, 156, 157].

1.13 Limitations

Despite being widely used, LMD is not without limitations. Successful application of LMD technology requires targeted applications of fixation, embedding, staining, and careful consideration of how these steps may affect downstream analyses. Modifying extraction procedures and downstream analyses may be necessary to account for fixative-induced alterations to biomolecules that can impede analysis and make performing LMD difficult. The following is an overview of limitations for LMD-based technology primarily associated with RNA targets and PCR analyses.

1.13.1 Fixation

The success of LMD is determined by the ability of the investigator to be able to discern one cell or tissue type from another via morphological characteristics. Fixation method is often a limiting factor of histological quality. Freezing tissues has long been thought of as the best way to preserve tissues for molecular analysis

because it involves no fixative solution that may alter the biochemical nature of the sample [17, 21]. However, frozen tissues often have less than desirable histological quality. Snap freezing, or the rapid freezing of tissues in liquid nitrogen, can cause the formation of ice crystals which can tear tissues and freezer burn may occur resulting in overall poor morphological quality [21, 158]. However, it is possible to improve both histological and molecular quality by freezing samples in a more controlled manner and by using Optimum Cutting Temperature (OCT) media and freezing tissues at a slower rate [21]. Other considerations for frozen samples include: storage of samples at -80°C , requiring space in an appropriate storage facility, can be cumbersome and expensive and sectioning of frozen tissues must be performed on a cryotome which may not be readily available [132].

An equally important factor in determining fixation method is how it will affect the biochemical and molecular qualities of the target biomolecule. As mentioned previously, freezing tissues allows for the preservation of structural and chemical characteristics of biomolecules such as DNA, RNA and proteins. Fixatives, such as formalin, preserve tissues by forming covalent bonds that cross-link proteins. This makes the extraction of acceptable quantity and quality nucleic acids or proteins difficult because cross-linking results in fragmented and chemically altered biomolecules. Formalin fixation has also proven to increase the aggregation of proteins like RNase and DNase in fixed tissues and this possibly accounts for some nucleic acid degradation [159]. Precipitating fixatives (alcohol-based) denature proteins and reduce the solubility of the tissue thus preserving tissue integrity. Biomolecules extracted from precipitating fixatives are more intact than those from

formalin-fixed tissues but are still more degraded than those from frozen tissues [160]. One study [161] evaluated effects of freezing, formalin fixation, and alcohol-based fixation on histological quality of tissue sections and RNA quantity and quality. It was determined that tissues frozen and embedded in OCT had exceptional quantity and quality RNA but had the poorest quality histological quality. Tissues fixed in formalin-based fixatives (10% neutral buffered formalin (NBF), Bouin's solution, Davidson's solution) had both reduced quantity and quality RNA but had exemplary histological quality [161]. Alcohol-based fixatives (70% ethanol, UMFIX, Carnoy's solution, methancarn) had good quantity and quality RNA and also had exemplary histological quality [160, 161]. Therefore, alcohol-based fixatives are the best choice of fixation for tissues to be used in downstream molecular analyses.

Duration of fixation is another determining step in the process. Good fixation is dependent on the ability of the fixative to penetrate the tissue and allowing time for the chemical reactions to take place [159]. Ideally, tissues will be placed in the fixative of choice as soon as possible following collection to reduce the buildup of nucleases and to prevent autolysis. Also important is the ratio of tissue to fixative. Keeping tissue pieces small in both size and number helps to ensure proper fixative penetration. Overfixation can aggravate the negative effects of various fixatives. A study by von Ahlfen et al., determined that overfixation in formalin, for example, may result in increased RNA fragmentation overtime [162].

1.13.2 Tissue Processing

How tissues are processed (i.e. embedded and stained) can also play a critical role in the quality of biomolecules extracted from fixed tissue. Two of the more common forms of embedding media are paraffin and plastic resin. Tissue sections embedded in resin have better histological detail than those embedded in paraffin, however, a special microtome is needed to section these tissues and special reagents are needed to clear the resin from the tissue during the staining process. Although it has been suggested that resin permits the extraction of higher integrity biomolecules, there is no data comparing paraffin and resin embedded tissues [20].

With the exception of immunohistochemical and *in situ* hybridization techniques, most staining for LMD is done to visualize histological characteristics. Staining methods may vary based on the target molecule but, typically, most tissues can be stained with general histological dyes. Because the area of LMD-excised tissues is so small there is little carryover of dye artifacts into downstream analysis [19]. For RNA extraction, it was found that using RNase-free dyes, less intense stains, and shorter protocols are best for recovering better quality RNA [158].

1.14 Procedural Adaptations

Fixed and embedded tissues have RNA fragments of 100-200 bases in length [163]. Most commonly used RNA extraction methods are not efficient at precipitating smaller fragments. Salts typically used for RNA precipitation like ammonium acetate are able to precipitate nucleic acids smaller than 100 basepairs (bp). Lithium chloride and sodium chloride are better for extracting small fragments

but chloride ions from these reagents can interfere with reverse transcriptases making analyses like qPCR difficult. Adding dilute concentrations of magnesium chloride to procedures using these salts can aid in small fragment precipitation. Even enzymes like the commonly used Proteinase K can have artifacts that carryover through the extraction procedure and interfere with reverse transcription [164]. Many companies have now designed nucleic acid isolation kits that target smaller fragments making the use of target molecules from LMD-derived tissues more obtainable [164-166].

The success of gene expression analyses like qPCR is dependent on the quality and quantity of the nucleic acid template [167] as well as the specificity and efficiency of the oligonucleotide primers [168]. In order to offset the fact that LMD results in poorer quality RNA, some adaptations to the assay are necessary including specialized primer design. Although RNA from fixed tissues typically ranges from 100-200 bases in length, designing primers with amplicons less than 100 bp has provided more robust data than primers with longer amplicons [169]. Other general principles for primer design include short primer length, staying within the optimal melting temperature range, and keeping the G/C content of the primers between 45-60% [168, 170]. Following this strategy will help insure that PCR reactions using LMD-derived target tissues will provide optimal and reliable data.

1.15 Summary and Implications

Postnatal uterine development involves a series of organizationally critical molecular and morphological changes. In the pig, gland genesis is an estrogen sensitive, ESR1-dependent event [33]. Estrogen driven morphogenesis and

cytodifferentiation of the endometrium are dependent on a complex network of stromal-epithelial interactions [46]. The proper formation of endometrial glands is essential to insure reproductive success in the adult female. Disruption of normal developmental events within the first two weeks of life in the pig results in reduced uterine capacity [2]. Data for RLX, a prototypical MbF in the pig, and temporospatial expression patterns of RXFP1 and ESR1 indicate that a lactocrine-driven mechanism for the onset of gland genesis exists between birth and PND 2 [4, 5, 11-13, 128]. In order to evaluate the cell-cell interactions influenced by lactocrine signaling a tool like LMD can be employed to isolate stroma and epithelium to allow cell compartment specific quantification of gene expression profiles. It was hypothesized that disrupting the course of development during the critical lactocrine programming window would result in altered gene expression profiles and result in an altered uterine phenotype [4]. Objectives of the first study presented below are to establish a working protocol for the use of LMD in evaluating effects of lactocrine signaling on cell-compartment specific gene expression events in the neonatal porcine endometrium. Objectives of the second study are to determine effects of nursing versus porcine milk-replacer feeding for two days from birth on patterns of endometrial compartment-specific *ESR1*, *RXFP1* and *VEGFA* expression and endometrial morphogenesis as determined on PND 2 and PND 14.

Chapter 2:

Laser Microdissection as a Tool to Evaluate Endometrial Cell-Compartment Specific Gene Expression in Fixed Tissues

2.1 Abstract

Laser microdissection (LMD), a tool originally developed to study cancer cells, has since been implemented in many life science fields. Cells are the functional unit of tissues. Understanding interactions between cells and their microenvironments is critical to understanding molecular processes associated with both tissue development and function. LMD is a tool that can be used to physically separate specific cell or tissue types from histological preparations. Once isolated, DNA, RNA, and proteins can be extracted from the targeted tissues or cells and biochemical analyses can be performed. Application of LMD for such purposes presents technical challenges. Among the most critical of such obstacles is tissue fixation which, depending upon the method, can affect both the quality and quantity of molecules extracted from fixed tissues. Due to the effects of fixative solutions on biomolecules, adaptations to extraction and analytical procedures may also be necessary. Here, LMD will be used to obtain physically pure stroma and epithelium in order to define patterns of gene expression in specific endometrial cell compartments on PND 2 and PND 14. Data indicate that RXFP1 is expressed primarily in porcine endometrial stroma at birth while ESR1 is not expressed in stroma until PND 2 and that expression patterns change over time. It is hypothesized that temporospatial

expression of these receptors mediate the onset of gland genesis in the neonatal porcine uterus. Understanding the compartment specific expression patterns will shed light on the stromal-epithelial interactions associated with uterine development.

2.2 Introduction

Laser microdissection, or laser-capture microdissection, was developed at the National Cancer Institute as a tool for understanding the microenvironments of tumor cell populations [18]. LMD allows for the isolation of single cell or groups of cells from within larger cell populations. Most LMD workstations can be adapted to excise regions of interest from histological preparations or live cell cultures [18, 134]. These isolated cells or groups of cells can then be used in downstream molecular analysis including qPCR. To date, LMD has been successfully applied in a wide range of fields including plant biology, clinical sciences, pathology, genomics, and developmental biology [137, 146, 148-150]. Despite the wide range of applications for LMD, it is not without limitations. In order to obtain high quality nucleic acids and proteins from fixed, embedded tissues targeted procedural adaptations are required.

Determining the appropriate fixation method is the first critical technical challenge. Formalin-based fixatives, like paraformaldehyde and neutral buffered formalin, preserve tissues by cross-linking proteins [161, 171]. This can result in extraction of both low quantity and poor quality target molecules [158]. Freezing tissues is considered the gold standard of fixation methods because this yields the highest quantity and quality biomolecules [161]. However, another consideration is

the histological quality of sections generated from fixed tissue. For LMD to be successful the researcher must be able to discern one cell population from another. During the freezing process ice crystals may form which can tear tissues and freezer burn may occur which can alter the morphological quality of the section [21]. This is not an issue with formalin-based fixatives which render high quality histological sections. Therefore, a fixative that provides the best molecular and histological quality possible is preferred. Alcohol-based fixatives, like Xpress Molecular Fixative (Sakura Finetek; Torrance, CA), have shown to provide molecular quality near that of frozen tissues as well as the histological quality of formalin-fixed tissues [160, 161, 172].

Extraction of nucleic acids, specifically RNA, from LMD-derived, fixed tissues is yet another consideration. Fixed, embedded tissues typically have RNA fragments of approximately 100-200 bases in length [159-161]. Commonly used extraction methods use salts that are not efficient at precipitating smaller RNA fragments and artifacts from extraction procedures can carryover and interfere with reverse transcription [164]. Commercially available RNA extraction kits that target fragmented RNA with little artifact carry over have made using RNA from fixed, embedded LMD-derived tissues more obtainable [166].

The success of gene expression analyses, like qPCR, depends first on the quality and quantity of the nucleic acid template and secondly, on the specificity and efficiency of the oligonucleotide primers [169]. Due to the less than ideal quality of RNA from LMD-derived specialized primer design may be required. Because RNA

fragments range from 100-200 bases in length, designing specific primers with amplicons of ≤ 100 base pairs will provide more robust data [169, 170].

Postnatal development of the porcine uterus involves a series of molecular and morphological changes between birth and PND 2 that are driven by stromal-epithelial interactions. Data show that stromal expression of RXFP1 from birth and onset of stromal ESR1 expression on PND 2 mediates the differentiation of epithelial cells in the neonatal porcine uterus [13, 33, 60]. Recently, a mechanism was proposed for the RXFP1-mediated, ESR1-dependent gene expression events that promote gland genesis in the neonatal porcine endometrium [4]. Disrupting these normal developmental events with the first two weeks of life can compromise the reproductive health of the adult [2, 9, 173]. Knowing how cell-compartment specific expression of ESR1 and RXFP1 changes overtime can shed light on how stromal-epithelial interactions mediate endometrial gland genesis. Here, objectives were to employ the use of LMD to evaluate gene expression profiles of RXFP1 and ESR1 in the porcine endometrium on PND 2 and PND 14.

2.3 Materials and Methods

Animals and Tissues

Gilts (n = 6-8/group) were assigned randomly at birth to one of two groups in which tissues were collected on i) PND 2 or ii) PND 14. Gilts were sedated and euthanized using Buthanasia-D Special (Intervet/Schering Plough Animal Health; Whitehouse Station, NJ). Uterine tissues were trimmed of excess connective tissue, fixed individually in Xpress Molecular Fixative (Sakura Finetek; Torrance, CA) and

embedded in Paraplast Plus (Fischer Scientific; Atlanta, GA). Uteri were sectioned at 10 μm thick (20-22 sections/animal) and mounted on Molecular Machines and Industries MembraneSlides (MMI; Haslett, MI).

Laser Microdissection

Whole uterine cross-sections were stained using a nuclease-free MMI H&E staining kit and were subjected to LMD using an MMI CellCut Laser Microdissection workstation. Target regions of interest, endometrial epithelium (LE and GE) and stroma, were identified and outlined using the MMI software. Epithelium and stroma were excised via the laser and isolated/captured on MMI IsolationCaps (Figure 1).

RNA Extraction/cDNA Synthesis

A Recoverall Total Nucleic Acid Isolation Kit (Ambion; Foster City, CA) was used to extract 300-500 ng of total RNA from 15 million μm^2 of isolated epithelium or stroma. Total RNA concentration was measured using a NanoDrop Spectrophotometer ND-1000. A High Capacity cDNA Reverse Transcriptase Kit (Applied Biosystems; Foster City, CA) was used to generate 500 ng of cDNA from 500 ng of total RNA.

Quantitative Real-time PCR

cDNA was used as template for quantification of *ESR1*, *RXFPI* and *S15* (reference gene) mRNA by qPCR. Procedures included use of Power SYBR Green PCR Master Mix (Applied Biosystems) and the Applied Biosystems Prism 7500. For

each transcript 10 ng of cDNA representing each sample were run in duplicate. Porcine-specific primers for *ESR1*, *RXFP1* and *S15* can be found in Table 1. Primers for *RXFP1* and *S15* were designed as described by Chen, et al. [128] and primers for *ESR1* was designed using Primer3 (www.primer3.sourceforge.com) and Amplify3 (www.engels.genetics.wisc.edu/amplify) software. Primers were designed to have product sizes of >100 bp.

Data Analysis

All quantitative data for qPCR results were subjected to analysis of variance using GLM procedures in the Statistical Analysis System. Data are presented as least squared means \pm standard errors (LSM \pm SEM).

2.4 Results

Validation of qPCR

For validation of qPCR procedures standard curves and dissociation curves were evaluated to determine primer efficiency and primer specificity (Figures 2 and 3). The slope of the standard curve for each target was used to calculate efficiency ($E = 10^{-1/\text{slope} - 1} \times 100$). Efficiencies for all targets on both PND 2 and PND 14 were between 85-115% indicating optimal amplification. For all targets, dissociation curves were evaluated to determine the melt profile, or melting point, of each sample. As demonstrated by the dissociation in curves in Figures 2 and 3 D, the profiles for all samples for each target consists of a single peak or melt point indicating high primer specificity.

Cell-compartment specific ESR1 mRNA expression

Data for ESR1 mRNA expression are presented in Figure 4. On PND 2, expression of ESR1 was highest ($P < 0.02$) in endometrial stroma. By PND 14, there was no difference seen in expression levels between epithelium and stroma.

Cell-compartment specific RXFP1 mRNA expression

Data for RXFP1 mRNA expression are presented in Figure 5. On PND 2, no difference was seen between stromal and epithelial RXFP1 expression. By PND 14, expression of RXFP1 was highest ($P < 0.002$) in the endometrial stroma.

2.5 Discussion

Data here show that LMD can be used to evaluate cell-compartment specific gene expression profiles from fixed, embedded neonatal porcine uterine tissue. The purpose of this report was to illustrate that procedural adaptations to fixation method, RNA extraction protocol, and primer design were essential to obtaining robust qPCR data. Tissues were fixed in Xpress Molecular Fixative which has been shown to preserve the integrity of RNA [160]. Uteri fixed in these tissues yielded adequate quality RNA to be used in qPCR analysis. The Ambion Total Nucleic Acid Isolation Kit is designed to extract fragmented RNA from fixed tissues. The use of this kit allowed for extraction of sufficient amounts of RNA. All primers for qPCR were designed to generate amplicons of less than 100 bp, with the exception of the high

abundance S15, due to the fragmented nature of RNA from fixed tissues [168, 169]. Evaluation of both standard and dissociation curves showed that designing the primers in this way allowed for optimal primer efficiency and specificity for each target. Guidelines from Bustin et al. [174] were used to validate qPCR data. Endometrial ESR1 mRNA expression patterns presented here agree with earlier reports that on PND 2 expression is primarily stromal [5, 8]. Expression patterns for RXFP1 mRNA also agree with immunolocalization of RXFP1 in the endometrial stroma on PND 14 [13].

Normal postnatal development, including the onset of gland genesis, in the porcine uterus is ESR1 dependent. At birth, the porcine uterus is ESR1-negative, but RXFP1 positive. It is believed that stromal RXFP1 mediates stromal expression of ESR1, as well as in nascent GE, by PND 2. These stromal-epithelial interactions drive postnatal uterine development, yet, are poorly understood. Using LMD as a tool to isolate these cell populations can provide new insight to the mechanisms that regulate cell-cell communication and microenvironments.

Gene	Accession no.	Forward	Reverse	Amplicon Size (bp)
<i>ESR1</i>	AF035775	TGATGATTGGTCTTGTCTGG	CCAGGAGCAAGTTAGGAGCAAA	70
<i>RXFP1</i>	CA994862	GCATCACTTTGAGGCAGAGACA	CCTCGGCAAAGACATTGCAT	69
<i>S15</i>	NM214334	GGTAGGTGTCTACAATGGCAAGG	GGCCGGCCATGCTTC	116

Table 1. Target porcine *ESR1*, *RXFP1*, and *S15* accession numbers, forward and reverse primers and amplicon size.

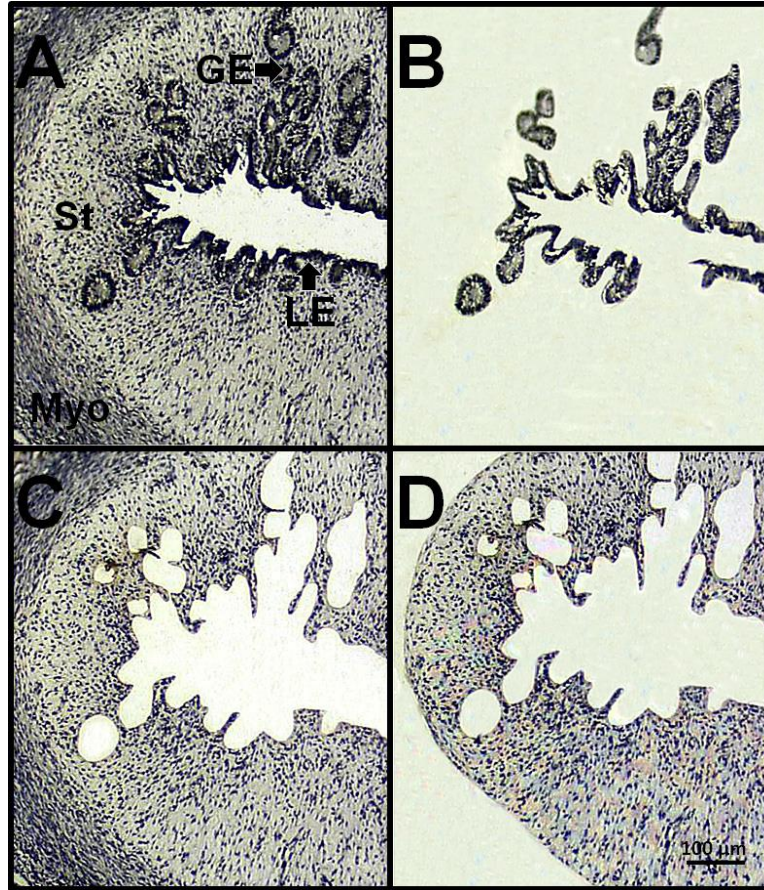


Figure 1. *Laser microdissection (LMD) of neonatal porcine endometrial stroma and epithelium.* Photomicrographs depict: an intact uterine cross section (A); excised, captured epithelium (B); the uterine cross section after excision of epithelium (C); and excised, captured endometrial stroma (D). GE = glandular epithelium. LE = luminal epithelium. St = endometrial stroma. Myo = myometrium.

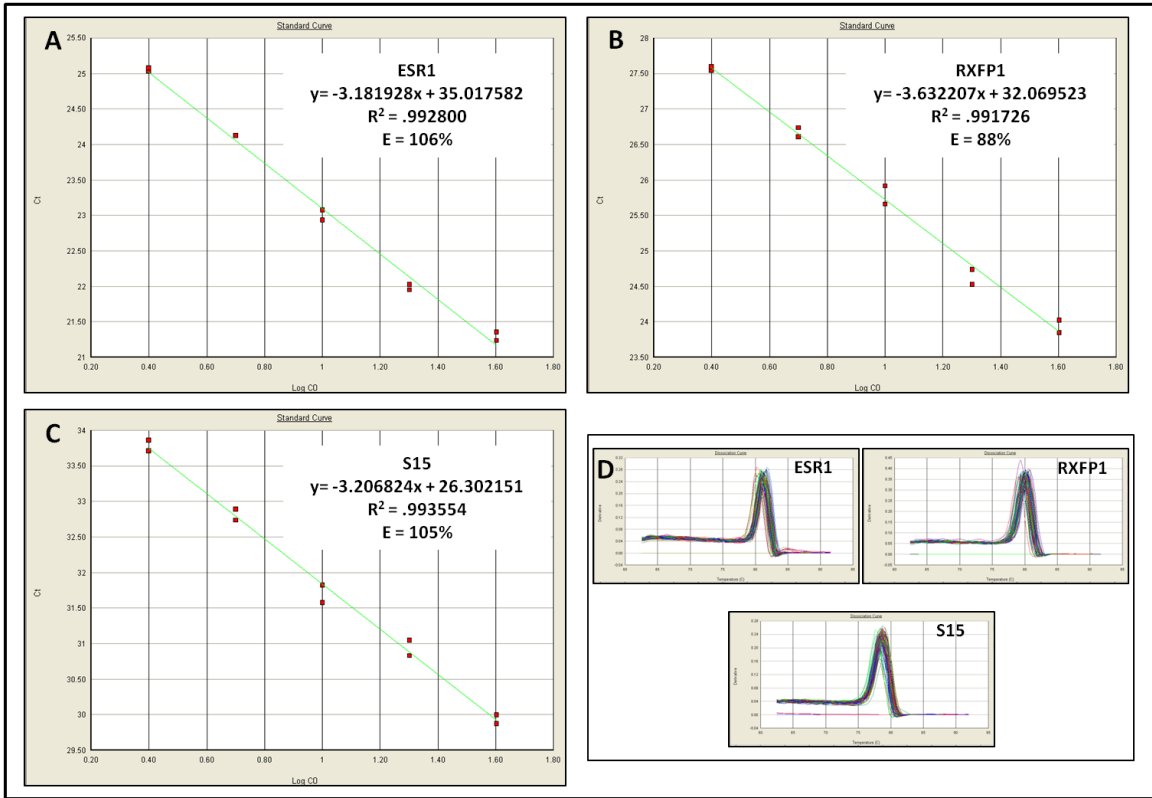


Figure 2. Validation of qPCR results in PND 2 endometrial samples. Shown here are standard curves for A) *ESR1*, B) *RXFP1*, and C) *S15* for PND 2 samples. Efficiencies (*E*) for all primers are between 85-115% and all $R^2 = .99$. Also shown (D) are dissociation curves for *ESR1*, *RXFP1*, and *S15* for all PND 2 samples. Single melt points on these curves indicate high primer specificity.

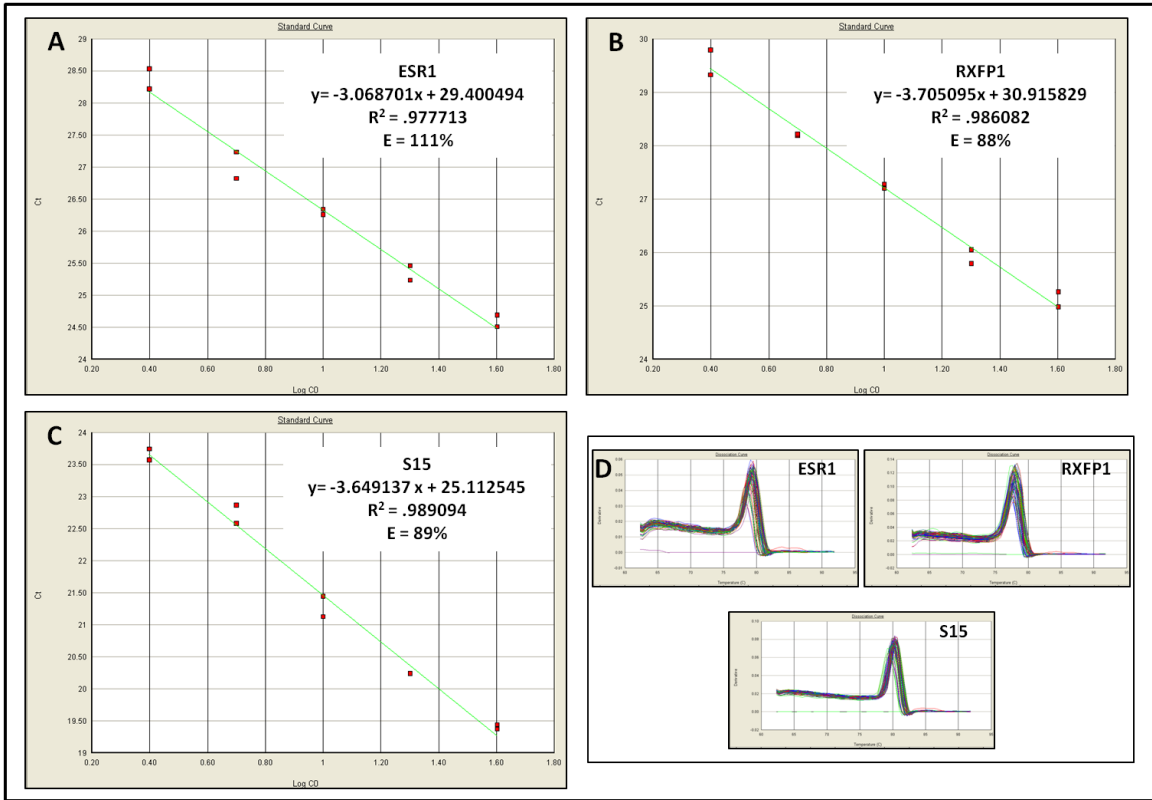


Figure 3. Validation of qPCR results in PND 14 endometrial samples. Shown here are standard curves for A) *ESR1*, B) *RXFP1*, and C) *S15* for PND 14 samples. Efficiencies (E) for all primers are between 85-115% and all $R^2 = .97 - .98$. Also shown are dissociation curves (D) for *ESR1*, *RXFP1*, and *S15* for all PND 2 samples. Single melt points on these curves indicate high primer specificity.

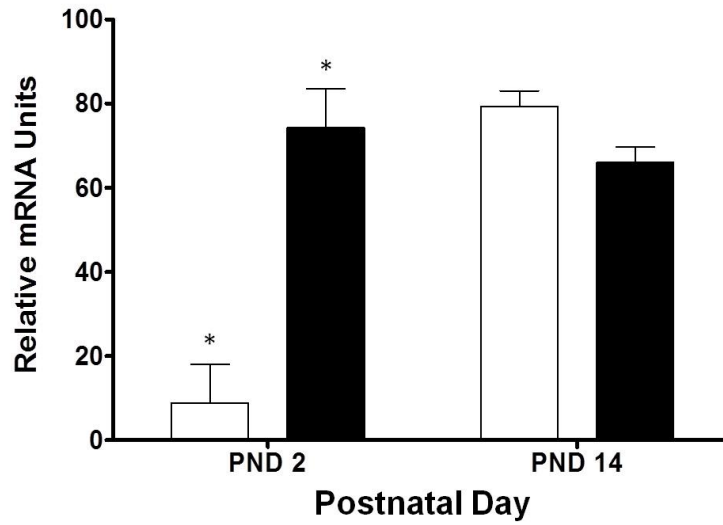


Figure 4. *Cell-compartment specific ESRI mRNA expression on PND 2 and PND 14.* On PND 2, *ESRI* mRNA expression was highest ($P < 0.02$) in the stroma and no differences were seen by PND 14. Open bars = epithelium and Closed bars = stroma. Asterisks denote differences.

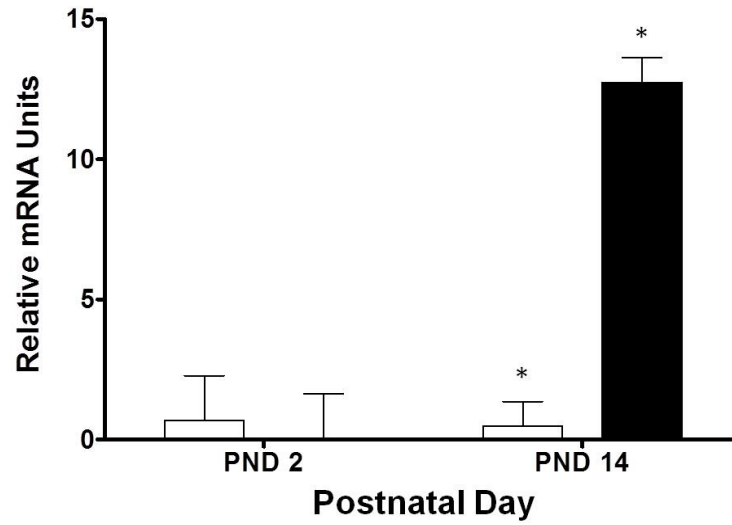


Figure 5. Cell-compartment specific *RXFP1* mRNA expression on PND 2 and PND 14. No differences were seen on PND 2. By PND 14, *RXFP1* mRNA expression was highest ($P < 0.002$) in endometrial stroma. Open bars = epithelium and Closed bars = stroma. Asterisks denote differences.

Chapter 3

Nursing for 48h from Birth Supports Porcine Uterine Gland Development and Endometrial Cell-Compartment Specific Gene Expression

3.1 Abstract

The first two weeks of neonatal life constitute a critical period for estrogen receptor-alpha (ESR1) -dependent uterine adenogenesis in the pig. A relaxin receptor (RXFP1) -mediated, lactocrine-driven mechanism was proposed to explain how nursing could regulate endometrial ESR1 and related gene expression events associated with adenogenesis in the porcine neonate during this period. To determine effects of nursing on endometrial morphogenesis and cell compartment-specific gene expression, gilts (n = 6-8/group) were assigned at birth to be either: A) nursed *ad libitum* for 48h; B) gavage-fed milk-replacer for 48h; C) nursed *ad libitum* to PND 14; or D) gavage-fed milk-replacer for 48h followed by *ad libitum* nursing to PND 14. Uteri were collected on PND 2 or PND 14. Endometrial histoarchitecture and both ESR1 and proliferating cell nuclear antigen (PCNA) labeling indices (LI) were evaluated. Laser microdissection was used to capture epithelium and stroma to evaluate treatment effects on cell compartment-specific *ESR1*, *VEGFA* and *RXFPI* expression. Imposition of a lactocrine-null state by milk replacer feeding for 48h from birth retarded endometrial development and adenogenesis. Effects of replacer feeding, evident by PND 2, were marked by PND 14 when endometrial thickness,

glandularity and gland depth were reduced. Consistently, in lactocrine-null gilts, PCNA LI was reduced in glandular epithelium (GE) and stroma on PND 14, when epithelial *ESR1* expression and ESR1 LI in GE were reduced and stromal *VEGFA* and *RXFPI* expression increased. Results establish that lactocrine signaling effects morphogenetic changes in developing uterine tissues that may determine reproductive capacity later in life.

3.2 Introduction

Lactation, the defining characteristic of mammals, involves production of milk by the mammary glands for delivery to offspring via nursing. Physiologically, lactation extends the time available for communication of nutrients and signaling molecules from mother to offspring into the postnatal period. Thus, nursing facilitates the fetal to neonatal transition and provides a mechanism for maternal and related environmental factors to affect neonatal growth and developmental programming [175-182]. The conserved nature of lactation [176, 177] suggests that transmission of nutrients and milk-borne bioactive factors (MbFs) from mother to offspring as a consequence of nursing has provided important adaptive advantages to mammals through lactocrine regulation [11, 60, 181, 182] of critical developmental events during neonatal life. While lactation strategies vary widely among mammals, milk consumption has broad implications for development that extend beyond basic nutritional support [176, 183, 184]. In marsupials, relationships between milk composition characteristic of multiple lactational stages and the state of development of nursing young are overt [117, 185, 186]. By contrast, such relationships are less

obvious in eutherian mammals, in which a single major change in milk composition is defined by the transition from production of colostrum (first milk) to milk early in lactation [176]. Still, peptide MbFs traverse the immature gastrointestinal (GI) tract and are delivered into the neonatal circulation [13, 14, 187]. It is clear that colostrum serves as a conduit for lactocrine transmission of signaling molecules [13, 16, 106, 111, 119, 175, 188-190]. Colostrum consumption affects differentiation of anterior pituitary mammotropes [187] and development of other somatic tissues including the GI tract, liver, kidney, spleen, muscle [15, 116, 117, 175, 191] and immune system maturation [108, 192-195].

Data for relaxin (RLX), a prototypical MbF in the domestic pig, indicate that a window of opportunity for lactocrine delivery of MbFs to offspring is open for approximately 48h from birth [13]. During this period the porcine endometrium undergoes organizationally critical, estrogen receptor-alpha (ESR1) -dependent cytodifferentiative and morphogenetic changes as glandular epithelium (GE) differentiates from luminal epithelium (LE) and nascent uterine glands begin to penetrate underlying stroma [5, 11, 33, 42, 60, 70]. Evidence for a lactocrine-driven, feed-forward mechanism regulating onset of ESR1 and vascular endothelial growth factor (VEGFA) expression in neonatal endometrium shortly after birth [127] suggested a role for lactocrine signaling in establishment of the neonatal uterine developmental program [60].

Recent studies of porcine uterine [128] and cervical [196] tissues showed that lactocrine signaling was required to support establishment of tissue-specific neonatal developmental programs, defined as the sequence of events that ultimately specify

cell fate and determine cell and tissue identify and function [196]. In these studies, nursing was shown to support normal expression patterns of key markers and mediators of uterine and cervical development including ESR1, VEGFA, and the RLX receptor, RXFP1. Moreover, data for whole cervical tissue [196] showed that disruption of lactocrine signaling for two days from birth (postnatal day = PND 0) by milk-replacer feeding induced changes in cervical protein and gene expression patterns at PND 2 that persisted to PND 14, even when replacer-fed gilts were returned to nursing at the end of PND 2. Effects included significant down-regulation of ESR1 protein expression. Observations indicated that lactocrine signaling is not only required to support the establishment of a normal development program, including patterns of uterine and cervical ESR1 expression, but may also determine the developmental trajectory of these female reproductive tract (FRT) tissues.

Disruption of estrogen-sensitive, ESR1-dependent organizational events associated with development of the neonatal porcine endometrium can have lasting effects on uterine function and reproductive performance in adults [33, 93]. Given that nursing is required to support the normal course of ESR1 and related gene expression events in the neonatal porcine uterus [128], it is reasonable to suggest that lactocrine signaling should be considered as an element of the organizational pallet of factors required to optimize uterine development and tissue developmental trajectory. The extent to which colostrum consumption affects uterine histogenesis and endometrial development has not been described. Moreover, lactocrine-sensitive, tissue compartment-specific developmental events [33] associated with programming of endometrial function remain to be defined. Therefore, to extend previous

observations on whole uterine tissue [197], this study was conducted to determine effects of nursing for two days from birth on: (1) endometrial histogenesis, including patterns of cell proliferation and *ESR1* expression *in situ*; and (2) temporospatial patterns of *RXFPI*, *ESR1* and *VEGFA* expression, using laser microdissection, at PND 2 and PND 14 in the neonatal pig.

3.3 Materials and Methods

Animals and Tissues

Crossbred gilts (*Sus scrofa domesticus*) (n = 6-8/group) were assigned randomly at birth to one of four treatment groups (Figure 6). Gilts were either: (1) nursed *ad libitum* for 48h; (2) gavage-fed commercial pig milk-replacer (Advance Baby Pig Liqui-Wean, Dundee, IL) for 48h (50ml/2h); (3) nursed *ad libitum* to PND 14; or (4) gavage-fed milk-replacer for 48h followed by return to *ad libitum* nursing on their dams to PND 14. Uteri were collected at 50h (PND 2; Groups 1 and 2) or on PND 14 (Groups 3 and 4). All procedures involving animals were reviewed and approved by Auburn University and Rutgers University Institutional Animal Care and Use Committees.

Uteri were trimmed of excess connective tissue, fixed individually in Xpress Molecular Fixative (Sakura Finetek; Torrance, CA) and embedded in Paraplast Plus (Fischer Scientific; Atlanta, GA). For laser microdissection, uterine cross-sections (10µm thickness, 20-22 sections/animal, n = 6-8 animals/group) were mounted on Molecular Machines and Industries MembraneSlides (MMI; Haslett, MI). For

immunohistochemistry and histomorphometry uterine cross-sections were cut at 6 μ m (4 sections/gilt) and mounted on glass slides.

Histomorphometry, immunohistochemistry (IHC) and image analysis

Tissue sections (n = 4 sections/gilt) were stained with hematoxylin. Histomorphometric measurements were obtained as described previously [35]. Briefly, endometrial thickness was measured as the distance from the base of the LE to the interface of the endometrium with inner circular myometrium. Gland penetration depth was measured from the basal aspect of LE defining the mouth of a gland to the distal tip of each gland where GE met stroma [35].

Immunohistochemistry was performed using a VectaStain Elite Kit (Vector Lab; Burlingame, CA). Four non-sequential sections per gilt were incubated overnight (4°C) with either mouse monoclonal anti-PCNA (Zymed/Invitrogen, 1:500), or with mouse monoclonal anti-ESR1 (DAKO; Carpinteria, CA; 1D5, 1:100). Negative control sections were incubated with mouse isotype control IgG (Zymed/Invitrogen; Carlsbad, CA). Following incubation with the secondary antibody and the ABC reagent, sections were developed with DAB (Sigma-Aldrich; St. Louis, MO).

Digital images of four endometrial areas per individual uterine section representing gilts from each treatment group were captured using a five megapixel QImaging camera. Images were taken at 10X using a 2.5X projection lens for ESR1 and a 3.3X projection lens for PCNA. Images were converted to grayscale and analyzed using ImageJ software (National Institute of Health; Bethesda, MD).

Digital images were converted to 8-bit greyscale and a generated look-up table was applied in order to link to pixel data and generate images with seven pseudocolor categories where each color represented a range of 36 pixel values. Colors were assigned automatically based on relative staining intensity of grayscale digital images. Nuclei were identified as positive when staining intensity values were at or above 30% of the highest values generated by ImageJ [42]. Thus, grayscale images were pseudocolored to illustrate relative staining intensity. Here, red-yellow color denotes positive staining. Using this protocol, images of negative control sections appear black. To determine labeling index (LI), a minimum of 1000 LE, GE, and stromal cells (labeled and unlabeled) were counted for each gilt. The number of labeled cells counted was divided by the total number of cells counted and multiplied by 100 to generate LI values, expressed as the percent of cells labeled [42].

Laser Microdissection, RNA extraction, cDNA synthesis and quantitative PCR (qPCR)

Uterine cross-sections, stained using an RNase-free, MMI hematoxylin Staining Kit, were subjected to LMD using an MMI CellCut Laser Microdissection workstation. Targeted regions of interest, including endometrial epithelium (LE and GE) and stroma, were identified and outlined using MMI software. Epithelium and stroma were then excised (Figure 1) and isolated/captured separately on RNase-free, MMI IsolationCaps.

The Recoverall Total Nucleic Acid Isolation Kit (Ambion; Foster City, CA) was used to extract 300-500ng of total RNA from $15 \times 10^6 \mu\text{m}^2$ of isolated epithelium

and stroma. Total RNA concentration was measured using an ND-1000 NanoDrop Spectrophotometer. The High Capacity cDNA Reverse Transcriptase Kit (Applied Biosystems; Foster City, CA) was used to generate an estimated 500ng of cDNA from 500ng of total RNA.

cDNA generated from isolated epithelial and stromal cells was used as a template for quantification of *ESR1*, *VEGFA*, *RXFPI* and *S15* (reference gene) mRNA by qPCR. Procedures included use of Power SYBR Green PCR Master Mix (Applied Biosystems) and an Applied Biosystems Prism 7500 qPCR system. For each transcript, a 10ng aliquot of cDNA representing each sample was run in duplicate. Primers for *RXFPI* and *S15* were designed as described by Chen, et al. [40] and primers for *ESR1* and *VEGFA* were designed using Primer3 (www.primer3.sourceforge.com) and Amplify3 (www.engels.genetics.wisc.edu/amplify) software. Primers were synthesized by Operon Biotechnologies (Huntsville, AL) and designed to have product sizes of less than 100 bp (Table 2). To insure specific amplification, tubes containing water only and primers with no template were included in each assay. Primer quality was evaluated by amplifying serial dilutions of the cDNA template. Dissociation curves were used to confirm primer specificity. Data were analyzed using the relative standard curve method for quantitation of gene expression as described by Applied Biosystems (ABI User Bulletin 2, 2001).

Statistical Analyses

All quantitative data for histomorphometry, IHC and qPCR were subjected to analyses of variance using GLM procedures in the Statistical Analysis System (SAS 2009-2010). Analyses considered variation due to the main effect of treatment (nursing vs replacer feeding) and, where appropriate, tissue compartment (epithelium vs stroma) for each day (PND 2 and PND 14). Error terms used in tests of significance were based on expectations of the mean squares for error. Data are presented as least squared means \pm standard errors (LSM \pm SEM).

3.4 Results

Endometrial histogenesis, cell proliferation and ESR1 labeling patterns

Effects of neonatal age and imposition of the lactocrine-null state by replacer feeding for two days from birth on endometrial histology are illustrated in Figure 7. Endometrial histology was similar in both nursed and replacer-fed gilts on PND 2, when nascent uterine glands, defined histologically as simple tubular epithelial structures beginning to penetrate the adluminal stroma, were apparent at intervals along the uterine luminal border (Figure 7A, B). Likewise, neither endometrial thickness nor uterine gland penetration depth differed between nursed and replacer-fed gilts on PND 2 (Figure 7C). In nursed gilts uterine gland genesis advanced from PND 2 to PND 14 (Figure 7 A vs D). When compared to gilts nursed for two weeks from birth, imposition of the lactocrine-null state for two days from birth retarded endometrial adenogenesis (Figure 7D vs E) and reduced both endometrial thickness ($P < 0.04$) and gland penetration depth ($P < 0.001$) on PND 14 (Figure 7F).

Images illustrating patterns of PCNA immunostaining and histograms summarizing PCNA LI data for endometrial LE, GE and stroma are presented in Figure 8. Signal indicative of PCNA labeling above background was observed most consistently in nascent GE on PND 2 (Figure 8A,B) and more regularly and distinctly in the distal tips of proliferating GE on PND 14 (Figure 8D,E). Consistently, PCNA LI was greater ($P < 0.01$) in GE than in LE or stroma on both PND 2 and PND 14 (Figure 8C,F).

Endometrial tissue compartment-specific effects on PCNA LI associated with imposition of the lactocrine-null state for two days from birth were observed on both PND 2 and PND 14. Compared with nursed controls, PCNA LI in replacer-fed gilts was reduced in both LE ($P < 0.02$) and GE ($P < 0.01$) on PND 2 (Figure 8C). On PND 14 (Figure 8F), PCNA LI in replacer-fed gilts was reduced in both GE ($P < 0.001$) and endometrial stroma ($P < 0.04$).

Images illustrating patterns of ESR1 immunostaining and histograms summarizing ESR1 LI data for endometrial LE, GE and stroma are presented in Figure 9. Signal indicative of ESR1 labeling above background was observed consistently in nascent (PND 2; Figure 9A,B) and proliferating (PND 14; Figure 9D,E) GE. On PND 2, ESR1 LI was greater in GE and stroma ($P < 0.001$) than in LE (Figure 9C). On PND 14, ESR1 LI was higher ($P < 0.001$) in GE than in either LE or stroma (Figure 9F).

Endometrial tissue compartment-specific effects on ESR1 LI associated with imposition of the lactocrine-null state for two days from birth were observed on both PND 2 and PND 14 (Figure 9C,F). In this case, stromal ESR1 LI was lower in

replacer-fed as compared to nursed controls on PND 2, whereas *ESR1* LI for GE was reduced ($P < 0.001$) in replacer-fed gilts on PND 14.

Endometrial tissue compartment-specific gene expression

Effects of treatment on endometrial epithelial and stromal compartment-specific expression of *ESR1*, *VEGFA* and *RXFPI* are illustrated in Figure 10. On PND 2, both *ESR1* (Figure 10A, $P < 0.002$) and *VEGFA* (Figure 10B, $P < 0.01$) expression was greater in endometrial stroma than epithelium, while *RXFPI* expression was greater (Figure 10C, $P < 0.001$) in epithelium than stroma. Imposition of the lactocrine-null state for two days from birth did not affect *ESR1* or *VEGFA* expression on PND 2 (Figures 10A,B). However, an endometrial tissue compartment-specific treatment effect was observed for *RXFPI*, where expression was greater ($P < 0.01$) in uterine epithelium of replacer-fed as compared to nursed gilts (Figure 10C, PND2).

On PND 14, *ESR1* expression was similar in epithelium and stroma (Figure 10A), whereas expression of both *VEGFA* ($P < 0.06$, Figure 10B) and *RXFPI* ($P < 0.04$, Figure 10C) was lower in endometrial epithelium. However, imposition of the lactocrine-null state for two days from birth reduced ($P < 0.02$) epithelial *ESR1* expression, and increased stromal expression of both *VEGFA* ($P < 0.003$) and *RXFPI* ($P < 0.04$) on PND 14 (Figure 10A-C).

3.5 Discussion

Earlier studies indicated that nursing is required for establishment of neonatal porcine uterine [197] and cervical [196] developmental programs between birth and PND 2. Present results confirm and extend those findings. Here, results show that imposition of the lactocrine-null state for two days from birth, by substituting milk replacer feeding for nursing, changed the uterine developmental program by PND 2 such that the developmental trajectory of the endometrium was altered at histomorphological, cellular and molecular levels on PND 14. These studies support and extend findings for the cervix [196], by showing that returning colostrum-deprived gilts to nursing after PND 2 failed to rescue uterine endometrial phenotype. Results provide evidence that lactocrine signaling during the first 48h of neonatal life triggers cell compartment-specific gene expression events and affects related cell behaviors that drive endometrial morphogenesis. Thus, lactocrine signaling contributes to the palette of factors affecting neonatal porcine uterine development.

Patterns of endometrial development observed for nursed gilts reflected those reported previously for the neonatal porcine uterus, as reviewed elsewhere [2]. Consistent with earlier observations [39, 42, 43, 70], differentiation of GE from LE, apparent on PND 2, as well as proliferation and development of nascent uterine glands were marked by intense, tissue site-specific PCNA and ESR1 immunostaining in GE that became more pronounced by PND 14. Patterns of cell proliferation reflected by PCNA immunostaining observed here were similar to those described for nascent uterine GE in the neonatal pig [43, 70], sheep [41] and mouse [198, 199].

Earlier studies showed that porcine uterine growth and histogenesis, reflected by systematic increases in uterine wet weight, endometrial and myometrial thickness

and patterns of adenogenesis between birth and PND 120, did not differ between gilts ovariectomized at birth and ovary-intact gilts prior to approximately PND 60, when ovarian factors begin to influence uterine growth [2, 39]. Thus, early events in postnatal development of the uterine wall do not require ovarian support. However, present results indicate that development of the porcine uterine wall during the period of ovary-independent uterine growth between birth and PND 14 does require lactocrine support. Effects of imposition of the lactocrine-null state for two days from birth on patterns of uterine wall development were pronounced. While endometrial histology characteristic of PND 2 was similar in nursed and replacer-fed gilts, uterine development was consistently and dramatically retarded in replacer-fed gilts by PND 14. Effects of imposition of the lactocrine-null state observed on PND 14 included reduced endometrial thickness and gland penetration depth, as well as marked inhibition of uterine gland development. This anti-adenogenic effect was similar to that observed for neonatal gilts treated with the anti-estrogen ICI 182,780 for two weeks from birth [70].

Data for PCNA LI, indicative of cell proliferation [200], revealed that nursing effects on endometrial development are evident by PND 2. Results were cell compartment-specific, showing that imposition of the lactocrine-null state from birth reduced PCNA LI in LE and GE on PND 2, and in GE and stroma at PND 14. Mechanistically, these observations are consistent with data indicating that endometrial thickness was reduced and uterine gland genesis was inhibited by PND 14 in the absence of lactocrine signaling from birth. Lactocrine effects on patterns of

cell proliferation suggest that mitogenic factors in colostrum are important for support of endometrial morphogenesis in the neonate [12, 14, 116].

Endometrial maturation and adenogenesis in the neonatal pig require ESR1 expression and activation of the estrogen receptor signal transduction system [70]. Undetectable at birth [39], porcine endometrial ESR1 expression was recently documented in both stroma and nascent GE for uterine tissues obtained at 24h postnatally [182] and is routinely identified by PND 2 [182, 197]. These observations were confirmed in the present study. Stromal ESR1 expression was observed most uniformly in nursed as compared to replacer-fed gilts at PND 2, when marked ESR1 expression was identified in nascent GE. Consistently, ESR1 LI, indicative of the percentage of ESR1-positive cells in a given category, was reduced in the endometrial stroma of replacer-fed gilts on PND 2. Results reinforce the observation that effects of nursing on endometrial development are detectable by PND 2. Patterns of adenogenesis and associated patterns of endometrial ESR1 expression observed to occur from PND 2 to PND 14 in nursed gilts also agree with previous observations [39, 70]. Advancement of uterine gland development during this period was expected to involve proliferation of ESR1-positive GE. However, in striking contrast to the normal condition identified for nursed gilts, marked inhibition of uterine adenogenesis induced by imposition of the lactocrine-null condition for two days from birth was associated with reduced epithelial *ESR1* mRNA expression and ESR1 LI for GE on PND 14.

Data presented here and elsewhere [197] indicate that normal ESR1 expression in the neonatal porcine uterus requires lactocrine support. A feed-forward,

lactocrine-driven mechanism was proposed [127] to explain how MbFs, exemplified by RLX, might support induction of endometrial ESR1 expression and related downstream effectors of estrogen and/or RLX action, including both VEGFA and RXFP1, in the neonatal porcine endometrium. Administered for two days from birth, exogenous RLX, a prototypical MbF in the pig [12], induced uterine expression of both ESR1 and VEGFA, and suppressed expression of RXFP1 [60]. Data indicating that uterotrophic effects of RLX can be inhibited with ICI 182,780 in neonatal gilts [60] and rats [201] suggests that ESR1 activation can occur indirectly, via transactivation of this receptor system. However, the extent to which RLX or other yet to be identified, lactocrine-active MbFs affect the state of ESR1 activation in the neonatal uterus is unknown.

It is clear that ESR1 activation is required to support uterine adenogenesis [202, 203]. Recently, the repressor of estrogen receptor activity (REA), a co-regulatory protein affecting function of the nuclear hormone-receptor complex, was implicated as an essential element of the mechanism regulating uterine adenogenesis in mice [203]. Adults rendered homozygous for the REA deletion (REAd/d) were infertile due to disruption of neonatal uterine adenogenesis, the consequent absence of uterine glands in adults, and related down-stream endometrial defects. However, adults rendered heterozygous for REA were hyper-responsive to estrogen. It was suggested that patterns of uterine development depend on REA gene dosage [203, 204]. Interestingly, the altered uterine phenotype in REAd/d mice was first observed developmentally between PND 10 and PND 14, a period associated with rapid gland genesis in this species [198, 205]. It will be important to determine the extent to

which lactocrine signaling affects REA expression or REA-mediated processes supporting uterine development in the neonatal pig.

Prior to this report, assessment of the effects of nursing on patterns of FRT development involved analysis of gene expression in uterine [197] and cervical [196] tissue extracts. Here, histological, IHC and LMD technologies were employed to determine effects of nursing on patterns of uterine wall development at histological, cellular and molecular levels. Immunohistochemical analyses enabled assessment of the temporospatial patterns of ESR1 expression and documentation of the percentage of cells in each endometrial compartment (LE, GE and stroma) labeled positively for nuclear ESR1 protein. Results of IHC-based analyses for ESR1 and ESR1 LI were generally complementary to those obtained by assessment of cell compartment-specific *ESR1* transcript expression. However, differences in relative expression of mRNA and protein can and do occur, as reported for uterine VEGFA and matrix metalloproteinase-9 in response to nursing at PND 2 [197].

It is well recognized that interactions between stroma and epithelium orchestrate development of the uterine wall [33, 46, 206, 207]. Thus, to understand how lactocrine signaling affects the porcine neonatal uterine developmental program, it is essential that effects of nursing on this process be defined on a cell compartment-specific basis. Here, LMD enabled physical dissection and capture of endometrial epithelial (LE + GE) and stromal cells from neonatal porcine uteri and evaluation of the effects of nursing versus imposition of the lactocrine-null condition for two days from birth on epithelial and stromal expression of *ESR1*, *VEGFA* and *RXFPI*. Isolation of LE and GE separately in sufficient quantities to enable evaluation of cell

type-specific responses for each epithelial cell compartment was not accomplished here. Thus, gene expression data based on the LMD protocol were obtained for total epithelium and stroma. Nevertheless, important relationships were identified that complement and extend earlier observations. For example, Chen et al [197], in a study of whole uterine tissue, reported that nursing for two days from birth increased *ESR1* expression when compared to gilts fed milk-replacer over the same period. Those results are consistent with the increase in *ESR1* expression in endometrial epithelium of nursed gilts observed in the present study at PND 14. On the other hand, as observed here for both epithelial and stromal cell compartments, *VEGFA* expression in whole uteri [197] was unaffected by nursing at PND 2. The increase in endometrial epithelial *RXFP1* expression observed for lactocrine-null gilts at PND 2 also agrees with observations reported for whole uteri 48h after colostrum deprivation from birth [197]. Since colostrum is a source of bioactive RLX [12], ingestion of RLX by nursing gilts may be acting in a negative regulatory manner to decrease *RXFP1* expression [60]. Data indicating that *RXFP1* expression is predominantly stromal agreed with an earlier report [13] in which both *RXFP1* mRNA and protein were localized primarily in this endometrial cell compartment at PND 14. Present data indicating increased stromal *RXFP1* expression for lactocrine-null gilts on PND 14 are consistent with those observations.

Temporospatial patterns of *ESR1* expression and ESR1 immunostaining illustrated here and elsewhere [39, 182] for neonatal porcine endometrium, suggest the evolution of paracrine conditions necessary to support stromal-epithelial interactions regulating endometrial adenogenesis and proliferation of nascent GE [7,

59, 208]. Results showing that endometrial *ESR1* expression is most pronounced in stroma of nursed gilts within two days of birth and increases in the epithelial compartment with differentiation of nascent, proliferating, ESR1-positive GE, agree with the idea that stromally derived ESR1-mediated signals support epithelial proliferation [59]. Thereafter, with differentiation and proliferation of nascent GE, reciprocal epithelial signals may affect endometrial cell viability by regulating organizationally important processes such as apoptosis [208, 209]. In this regard, imposition of the lactocrine-null state for two days from birth suppressed expression of the anti-apoptotic factor B-cell lymphoma-2 in neonatal cervical tissues on both PND 2 and PND 14 [196]. To the extent that similar events occur in the developing endometrium, such conditions could destabilize GE and uterine gland development. Reduced epithelial *ESR1* expression and ESR1 LI observed for GE was accompanied by parallel reductions in PCNA LI, observed for both GE and stroma, as well as altered patterns of expression documented for stromal *VEGFA* and *RXFPI* on PND 14 in replacer-fed gilts. Dysregulation of both stromal *VEGFA* and *RXFPI* expression by PND 14 in replacer-fed gilts suggests further disintegration of adenogenic conditions [127]. These relationships reinforce the idea that a lactocrine-driven paracrine regulatory system supportive of endometrial development evolves between birth and PND 14.

Lactocrine signaling is clearly required for establishment of the normal porcine endometrial developmental program and imposition of the lactocrine-null state from birth affects the trajectory of endometrial development in the neonate. If the lactocrine hypothesis is correct, disruption of lactocrine signaling would be

predicted to have long-term consequences for uterine function and fecundity. In a recent report [182], the relationship between PND 0 immunoglobulin immunocrit, a measure of colostrum intake by neonatal piglets [210], and litter size was defined using data for 381 gilts over four parities (approximately 1525 litters). As predicted by the lactocrine hypothesis, results showed that low immunocrit, indicative of minimal colostrum consumption on PND 0, was associated significantly with reduced litter size in adulthood. These data provide compelling support for the idea that colostrum consumption from birth and, therefore, lactocrine signaling affects uterine capacity and reproductive performance in adults.

Present data establish the importance of lactocrine signaling as an effector of organizationally critical structural changes in developing uterine tissues that can determine reproductive capacity later in life. Observations indicating that effects of nursing on neonatal endometrial development can be tissue compartment-specific point to the importance of stromal-epithelial interactions as determinants of uterine developmental trajectory. Efforts to understand how lactocrine signaling affects establishment of the uterine developmental epigenotype [182] will provide important insights into maternal programming of reproductive performance and health.

	Accession no.	Forward	Reverse	Amplicon Size (bp)
<i>ESRI</i>	AF035775	TGATGATTGGTCTTGTCTGG	CCAGGAGCAAGTTAGGAGCAAA	70
<i>VEGFA</i>	AF318502	AAGATCCGCAGACGTGTAAG	CACATCTGCAAGTACGTTTCG	93
<i>RXFPI</i>	CA994862	GCATCACTTTGAGGCAGAGACA	CCTCGGCAAAGACATTGCAT	69
<i>S15</i>	NM214334	GGTAGGTGTCTACAATGGCAAGG	GGCCGGCCATGCTTC	116

Table 2. Targeted porcine gene accession numbers, forward and reverse primer sequences and predicted amplicon sizes.

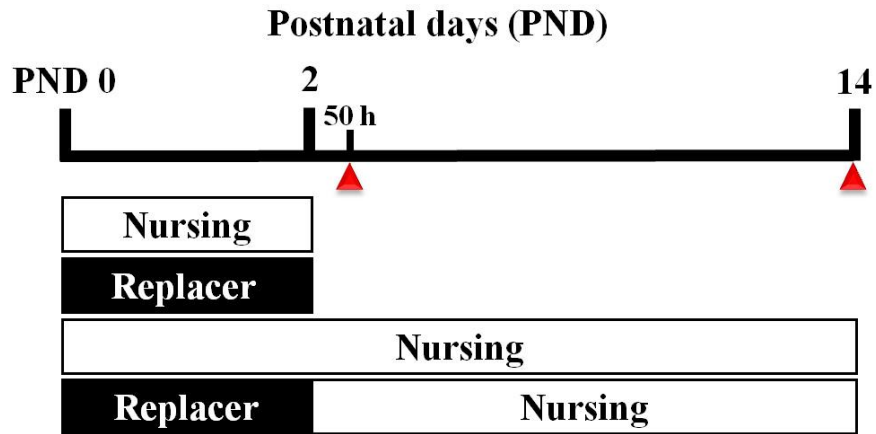


Figure 6. *Experimental Design.* Gilts (n = 6-8/group) were assigned randomly at birth (PND 0) to one of four treatment groups in which gilts were either: (1) nursed *ad libitum* for 48h; (2) gavage-fed commercial sow milk-replacer for 48h; (3) nursed *ad libitum* to PND 14; or (4) gavage-fed milk-replacer for 48h followed by *ad libitum* nursing to PND 14. Uteri were collected at 50h or on PND 14 (indicated by red arrows).

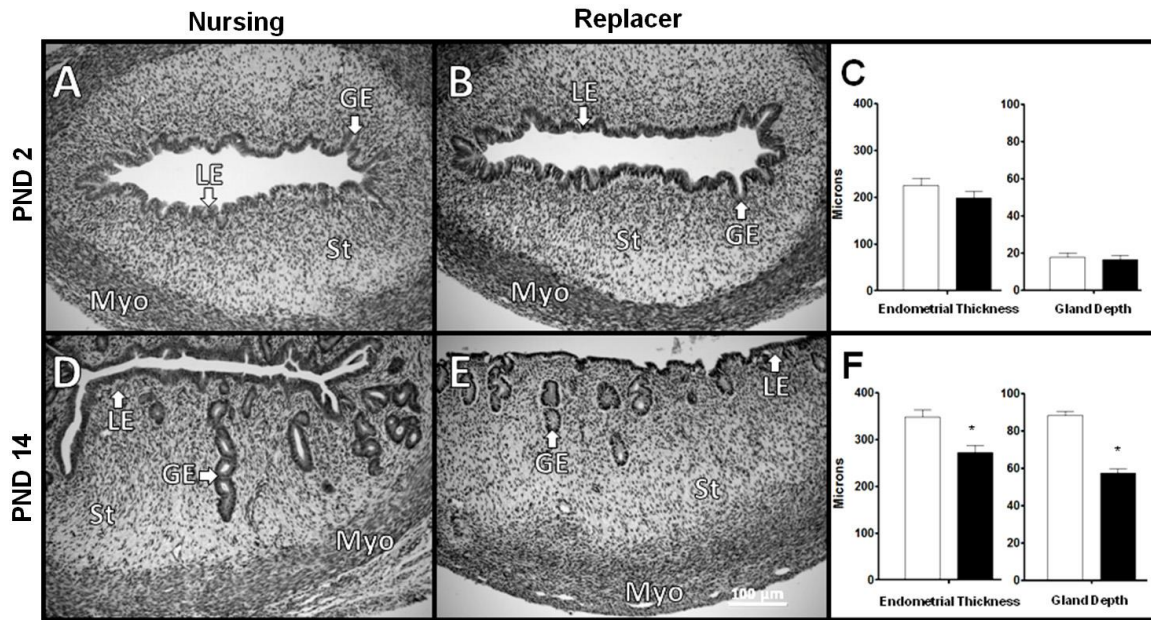


Figure 7. *Endometrial histoarchitecture affected by age and nursing.* Photomicrographs of hematoxylin stained tissue sections depict uterine histoarchitecture on PND 2 (A,B) and 14 (D,E) in nursed (A,D) and replacer-fed (B,E) gilts. On PND 2 (C), gland penetration depth and endometrial thickness were not affected by imposition of the lactocrine-null state. By PND 14 (F), gland depth ($P < 0.0001$) and endometrial thickness ($P < 0.04$) were reduced in replacer-fed gilts. Overall, imposition of the lactocrine-null state for 48h from birth retarded endometrial development by PND 14 (D vs E). For histograms (C,F): Open bars = nursed, Closed bars = replacer-fed; asterisks denote histological differences as indicated.

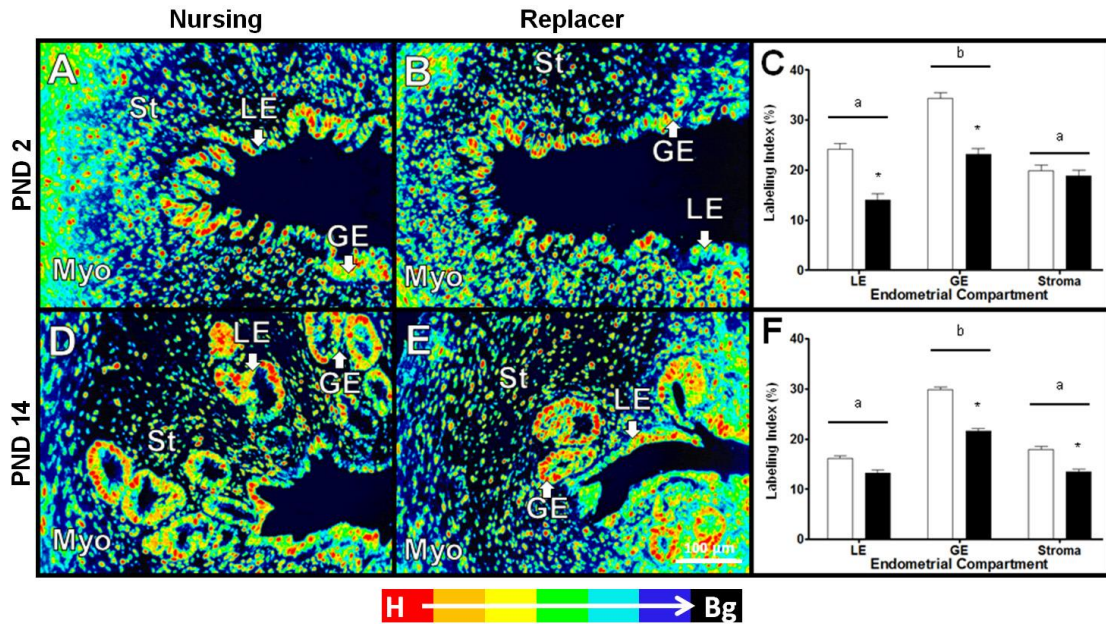
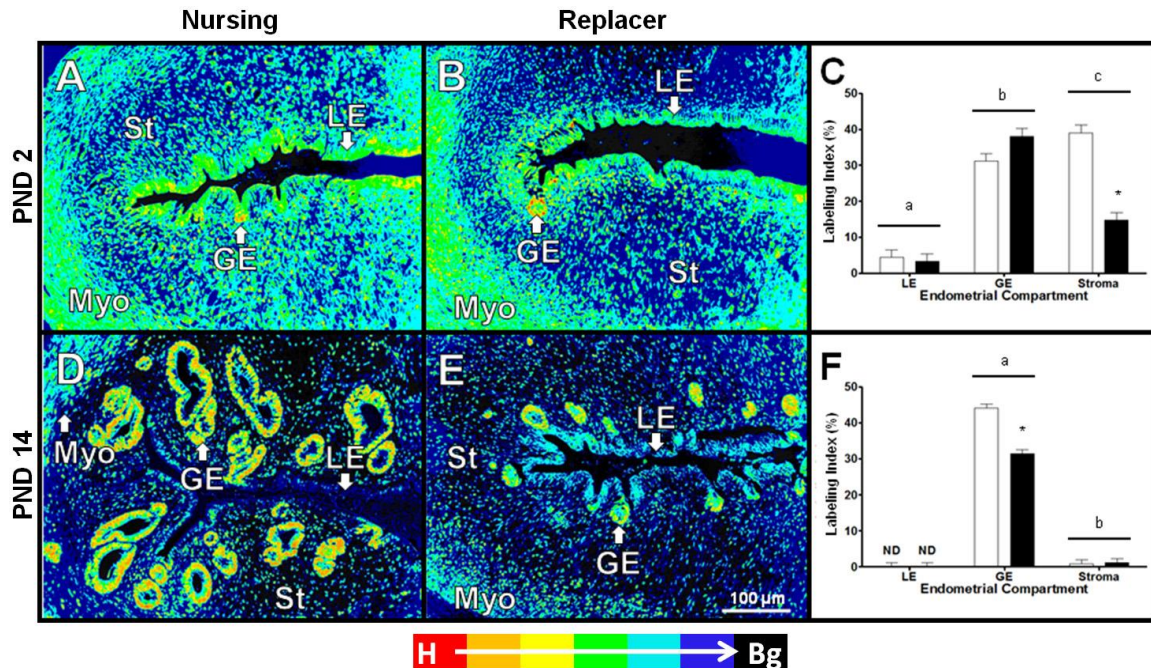


Figure 8. Endometrial PCNA immunostaining and labeling indices affected by neonatal age and nursing. Pseudocolored images depict PCNA immunostaining for PND 2 (A,B) and 14 (D,E) in nursed (A,D) and replacer-fed (B,E) gilts. Nuclei of cells staining positively appear yellow-red. Blue-black color denotes background. On PND 2 (C), PCNA LI was greater ($P < 0.002$) in GE than in LE and stroma. PCNA LI was reduced in both LE ($P < 0.02$) and GE ($P < 0.01$) of replacer-fed gilts on PND 2. On PND 14 (F), PCNA LI remained greater ($P < 0.0001$) in GE than in LE and stroma, and was reduced in GE ($P < 0.0002$) and stroma ($P < 0.04$) in replacer-fed gilts. Signal intensity is indicated by color (bottom legend: H = high to Bg = background). For histograms (C,F): Open bars = nursed, Closed bars = replacer-fed. On a within-day basis, cell compartments (LE, GE, stroma) denoted by



horizontal lines with different letters differ. Asterisks denote treatment differences within cell compartments. See text for detailed descriptions of these relationships.

Figure 9. Endometrial ESR1 immunostaining and labeling indices affected by neonatal age and nursing. Pseudocolored images depict nuclear ESR1 immunostaining for PND 2 (A,B) and 14 (D,E) in nursed (A,D) versus replacer-fed (B,E) gilts. Nuclei of cells staining positively appear yellow-red. Blue-black color denotes background. Uterine gland development advanced from PND 2 to 14 (A vs D), but was markedly retarded in replacer-fed gilts by PND 14 (D vs E). On PND 2, ESR1 LI was greater in GE ($P < 0.0001$) and stroma ($P < 0.0001$) than LE. Stromal ESR1 LI was reduced ($P < 0.001$) in replacer-fed gilts on PND 2 (C). On PND 14 (F), ESR1 LI was higher ($P < 0.001$) in GE than stroma. Glandular epithelial ESR1 LI was reduced ($P < 0.0001$) in replacer gilts on PND 14. Signal intensity is indicated by

color (bottom legend: H = high to Bg = background). For histograms (C,F): Open bars = nursed, Closed bars = replacer-fed. On a within-day basis, cell compartments (LE, GE, stroma) denoted by horizontal lines with different letters differ. Asterisks denote treatment differences within cell compartments. See text for detailed descriptions of these relationships.

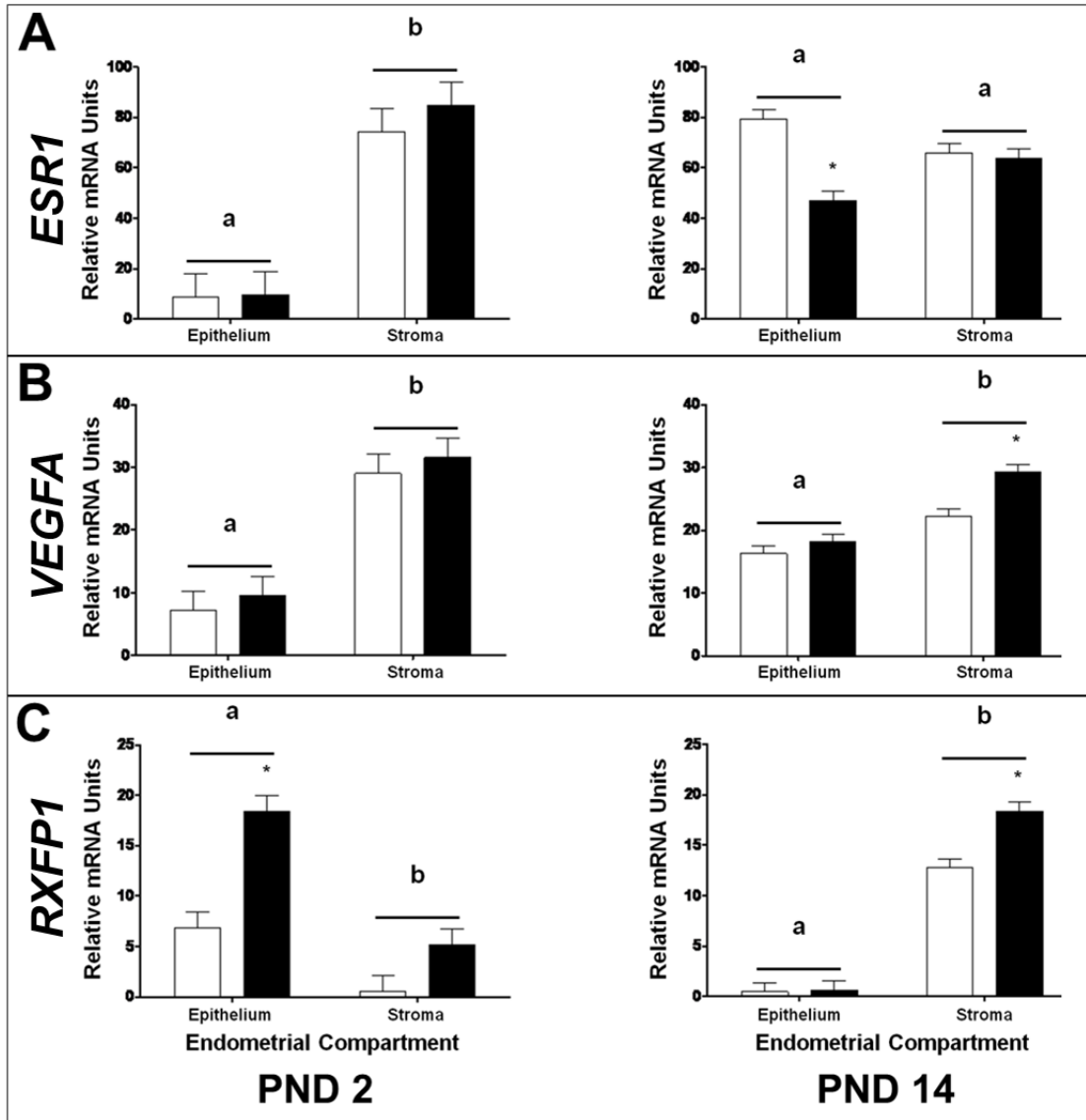


Figure 10. Endometrial tissue compartment-specific expression of *ESR1* (A), *VEGFA* (B) and *RXFP1* (C) mRNA on PND 2 (left) and PND 14 (right) in gilts nursed (open bars) or fed milk replacer (closed bars) for two days from birth. On a within-day basis, cell compartments (epithelium vs stroma) denoted by horizontal lines with different letters differ. Asterisks denote treatment differences within cell compartments. See text for detailed descriptions of these relationships.

References

1. Senger P. Pathways to Pregnancy and Parturition. Pullman: Current Conceptions, Inc; 2003.
2. Bartol FF, Wiley AA, Spencer TE, Vallet JL, Christenson RK. Early Uterine Development in Pigs. *Journal of Reproduction and Fertility* 1993; 48 (Suppl):99-116.
3. Spencer TE, Hayashi K, Hu J, Carpenter KD. Comparative developmental biology of the mammalian uterus. In: *Curr Top Dev Biol*, vol. 68. United States; 2005: 85-122.
4. Bartol FF, Wiley AA, Bagnell CA. Epigenetic programming of porcine endometrial function and the lactocrine hypothesis. *Reproduction in Domestic Animals* 2008; 43:273-279.
5. Yan W, Ryan PL, Bartol FF, Bagnell CA. Uterotrophic effects of relaxin related to age and estrogen receptor activation in neonatal pigs. *Reproduction* 2006; 131:943-950.
6. Gray CA, Bartol FF, Tarleton BJ, Wiley AA, Johnson GA, Bazer FW, Spencer TE. Developmental biology of uterine glands. *Biology of Reproduction* 2001; 65:1311-1323.
7. Bigsby RM. Control of growth and differentiation of the endometrium: the role of tissue interactions. *Ann N Y Acad Sci* 2002; 955:110-117; discussion 118, 396-406.

8. Spencer TE, Wiley AA, Bartol FF. Neonatal age and period of estrogen exposure affect porcine uterine growth, morphogenesis, and protein synthesis. *Biol Reprod* 1993; 48:741-751.
9. Bartol FF, Wiley AA, Floyd JG, Ott TL, Bazer FW, Gray CA, Spencer TE. Uterine differentiation as a foundation for subsequent fertility. *Journal of Reproduction and Fertility* 1999:287-302.
10. Tarleton BJ, Braden TD, Wiley AA, Bartol FF. Estrogen-induced disruption of neonatal porcine uterine development alters adult uterine function. *Biology of Reproduction* 2003; 68:1387-1393.
11. Bagnell CA, Steinetz BG, Bartol FF. Milk-borne relaxin and the lactocrine hypothesis for maternal programming of neonatal tissues. *Ann N Y Acad Sci* 2009; 1160:152-157.
12. Frankshun A-L, Ho T-Y, Reimer DC, Chen J, Lasano S, Steinetz BG, Bartol FF, Bagnell CA. Characterization and biological activity of relaxin in porcine milk. *Reproduction* 2011; 141:373-380.
13. Yan W, Wiley AA, Bathgate RA, Frankshun AL, Lasano S, Crean BD, Steinetz BG, Bagnell CA, Bartol FF. Expression of LGR7 and LGR8 by neonatal porcine uterine tissues and transmission of milk-borne relaxin into the neonatal circulation by suckling. *Endocrinology* 2006; 147:4303-4310.

14. Blum JW, Baumrucker CR. Insulin-like growth factors (IGFs), IGF binding proteins, and other endocrine factors in milk: role in the newborn. *Adv Exp Med Biol* 2008; 606:397-422.
15. Burrin DG, Davis TA, Ebner S, Schoknecht PA, Fiorotto ML, Reeds PJ, McAvoy S. Nutrient-independent and nutrient-dependent factors stimulate protein synthesis in colostrum-fed newborn pigs. *Pediatr Res* 1995; 37:593-599.
16. Playford RJ, Macdonald CE, Johnson WS. Colostrum and milk-derived peptide growth factors for the treatment of gastrointestinal disorders. *Am J Clin Nutr* 2000; 72:5-14.
17. Bonner RF, Emmert-Buck M, Cole K, Pohida T, Chuaqui R, Goldstein S, Liotta LA. Laser capture microdissection: molecular analysis of tissue. *Science* 1997; 278:1481,1483.
18. Emmert-Buck MR, Bonner RF, Smith PD, Chuaqui RF, Zhuang Z, Goldstein SR, Weiss RA, Liotta LA. Laser capture microdissection. *Science* 1996; 274:998 - 1001.
19. Ehrig T, Abdulkadir SA, Dintzis SM, Milbrandt J, Watson MA. Quantitative amplification of genomic DNA from histological tissue sections after staining with nuclear dyes and laser capture microdissection. *J Mol Diagn* 2001; 3:22-25.
20. Fink L, Bohle RM. Laser microdissection and RNA analysis. *Methods Mol Biol* 2005; 293:167-185.

21. Huang LE, Luzzi V, Ehrig T, Holtschlag V, Watson MA. Optimized tissue processing and staining for laser capture microdissection and nucleic acid retrieval. *Methods Enzymol* 2002; 356:49-62.
22. Aigner B, Renner S, Kessler B, Klymiuk N, Kurome M, Wunsch A, Wolf E. Transgenic pigs as models for translational biomedical research. *J Mol Med (Berl)* 2010; 88:653-664.
23. Fan B, Gorbach DM, Rothschild MF. The pig genome project has plenty to squeal about. *Cytogenet Genome Res* 2011; 134:9-18.
24. Foxcroft GR, Dixon WT, Novak S, Putman CT, Town SC, Vinsky MD. The biological basis for prenatal programming of postnatal performance in pigs. In: *J Anim Sci*, vol. 84 Suppl. United States; 2006: E105-112.
25. Telugu BP, Ezashi T, Roberts RM. The promise of stem cell research in pigs and other ungulate species. *Stem Cell Rev* 2010; 6:31-41.
26. Xiangdong L, Yuanwu L, Hua Z, Liming R, Qiuyan L, Ning L. Animal models for the atherosclerosis research: a review. *Protein Cell* 2011; 2:189-201.
27. National Pork Producers Council; www.nppc.org. 2011.
28. Pork Production; US EPA. In: U.S. Dept. of Agriculture/Dept. of Health and Human Services; www.epa.gov/agriculture/ag101/printpork.html. 2011.
29. Schook L, Beattie C, Beaver J, Donovan S, Jamison R, Zuckermann F, Niemi S, Rothschild M, Rutherford M, Smith D. Swine in biomedical research: creating the building blocks of animal models. *Anim Biotechnol* 2005; 16:183-190.

30. Geisert R. Pigs. In: Knobil (ed.) *Encyclopedia of Reproduction*, vol. 3. San Diego, London, Boston, New York, Sydney, Tokyo, Toronto: Academic Press; 1999: 792-799.
31. Kobayashi A, Behringer RR. Developmental genetics of the female reproductive tract in mammals. In: *Nat Rev Genet*, vol. 4. England; 2003: 969-980.
32. Orvis GD, Behringer RR. Cellular mechanisms of Müllerian duct formation in the mouse. *Developmental Biology*; 306.
33. Bartol FF, Wiley AA, Bagnell CA. Uterine development and endometrial programming. In: Asworth CJ, Kraeling RR (eds.), *Control of Pig Reproduction VII*: Nottingham University Press, UK; 2006: 113-130.
34. Kurita T, Cooke PS, Cunha GR. Epithelial-stromal tissue interaction in paramesonephric (Mullerian) epithelial differentiation. *Dev Biol* 2001; 240:194-211.
35. Bartol F. Uterus, nonhuman. In: Bazer F (ed.) *Encyclopedia of Reproduction*; 1998.
36. Amoroso EC. Placentation. In: Parkes A (ed.) *Marshall's Physiology of Reproduction*, vol. 2, 3rd ed. London: Longmans Green; 1952: 127-311.
37. Bazer FW. Uterine protein secretions: Relationship to development of the conceptus. *J Anim Sci* 1975; 41:1376-1382.
38. Roberts RM, Bazer FW. The functions of uterine secretions. *J Reprod Fertil* 1988; 82:875-892.

39. Tarleton BJ, Wiley AA, Spencer TE, Moss AG, Bartol FF. Ovary-independent estrogen receptor expression in neonatal porcine endometrium. *Biology of Reproduction* 1998; 58:1009-1019.
40. Brody JR, Cunha GR. Histologic, morphometric, and immunocytochemical analysis of myometrial development in rats and mice: I. Normal development. *Am J Anat* 1989; 186:1-20.
41. Bartol FF, Wiley AA, Coleman DA, Wolfe DF, Riddell MG. Ovine uterine morphogenesis: effects of age and progestin administration and withdrawal on neonatal endometrial development and DNA synthesis. *Journal of Animal Science* 1988; 66:3000-3009.
42. Masters RA, Crean BD, Yan W, Moss AG, Ryan PL, Wiley AA, Bagnell CA, Bartol FF. Neonatal porcine endometrial development and epithelial proliferation affected by age and exposure to estrogen and relaxin. *Domest Anim Endocrinol* 2007; 33:335-346.
43. Spencer TE, Bartol FF, Wiley AA, Coleman DA, Wolfe DF. Neonatal porcine endometrial development involves coordinated changes in DNA synthesis, glycosaminoglycan distribution, and ³H-glucosamine labeling. *Biol Reprod* 1993; 48:729-740.
44. Dziuk PJ, Gehlbach GD. Induction of Ovulation and Fertilization in the Immature Gilt. *J. Anim Sci.* 1966; 25:410-413.
45. Gray CA, Taylor KM, Bazer FW, Spencer TE. Mechanisms regulating norgestomet inhibition of endometrial gland morphogenesis in the neonatal ovine uterus. *Molecular Reproduction and Development* 2000; 57:67-78.

46. Cunha GR. Stromal induction and specification of morphogenesis and cytodifferentiation of the epithelia of the Mullerian ducts and urogenital sinus during development of the uterus and vagina in mice. *J Exp Zool* 1976; 196:361-370.
47. Lejeune B, Van Hoek J, Leroy F. Transmitter role of the luminal uterine epithelium in the induction of decidualization in rats. *J Reprod Fertil* 1981; 61:235-240.
48. Cunha GR, Cooke PS, Kurita T. Role of stromal-epithelial interactions in hormonal responses. *Arch Histol Cytol* 2004; 67:417-434.
49. Toft D, Gorski J. A receptor molecule for estrogens: isolation from the rat uterus and preliminary characterization. *Proc Natl Acad Sci U S A* 1966; 55:1574-1581.
50. Toft D, Shyamala G, Gorski J. A receptor molecule for estrogens: studies using a cell-free system. *Proc Natl Acad Sci U S A* 1967; 57:1740-1743.
51. Dahlman-Wright K, Cavailles V, Fuqua SA, Jordan VC, Katzenellenbogen JA, Korach KS, Maggi A, Muramatsu M, Parker MG, Gustafsson JA. International Union of Pharmacology. LXIV. Estrogen receptors. In: *Pharmacol Rev*, vol. 58. United States; 2006: 773-781.
52. Jensen EV, Jordan VC. The estrogen receptor: a model for molecular medicine. *Clin Cancer Res* 2003; 9:1980-1989.
53. Maggiolini M, Picard D. The unfolding stories of GPR30, a new membrane-bound estrogen receptor. *J Endocrinol* 2010; 204:105-114.

54. Carley ME, Rickard DJ, Gebhart JB, Webb MJ, Podratz KC, Spelsberg TC. Distribution of estrogen receptors alpha and beta mRNA in mouse urogenital tissues and their expression after oophorectomy and estrogen replacement. *Int Urogynecol J Pelvic Floor Dysfunct* 2003; 14:141-145.
55. Couse JF, Lindzey J, Grandien K, Gustafsson JA, Korach KS. Tissue distribution and quantitative analysis of estrogen receptor-alpha (ERalpha) and estrogen receptor-beta (ERbeta) messenger ribonucleic acid in the wild-type and ERalpha-knockout mouse. *Endocrinology* 1997; 138:4613-4621.
56. Krege JH, Hodgin JB, Couse JF, Enmark E, Warner M, Mahler JF, Sar M, Korach KS, Gustafsson JA, Smithies O. Generation and reproductive phenotypes of mice lacking estrogen receptor beta. *Proc Natl Acad Sci U S A* 1998; 95:15677-15682.
57. Greco TL, Furlow JD, Duello TM, Gorski J. Immunodetection of estrogen receptors in fetal and neonatal female mouse reproductive tracts. *Endocrinology* 1991; 129:1326-1332.
58. Greco TL, Duello TM, Gorski J. Estrogen receptors, estradiol, and diethylstilbestrol in early development: the mouse as a model for the study of estrogen receptors and estrogen sensitivity in embryonic development of male and female reproductive tracts. *Endocr Rev* 1993; 14:59-71.
59. Cooke PS, Buchanan DL, Young P, Setiawan T, Brody J, Korach KS, Taylor J, Lubahn DB, Cunha GR. Stromal estrogen receptors mediate mitogenic effects of estradiol on uterine epithelium. *Proc Natl Acad Sci U S A* 1997; 94:6535-6540.

60. Yan W, Chen J, Wiley AA, Crean-Harris BD, Bartol FF, Bagnell CA. Relaxin (RLX) and estrogen affect estrogen receptor-alpha, vascular endothelial growth factor and RLX receptor expression in the neonatal porcine uterus and cervix. *Reproduction* 2008; 135:705-712.
61. Yao L, Agoulnik AI, Cooke PS, Meling DD, Sherwood OD. Relative roles of the epithelial and stromal tissue compartment(s) in mediating the actions of relaxin and estrogen on cell proliferation and apoptosis in the mouse lower reproductive tract. *Ann N Y Acad Sci* 2009; 1160:121-129.
62. Miller C, Pavlova A, Sassoon DA. Differential expression patterns of Wnt genes in the murine female reproductive tract during development and the estrous cycle. *Mech Dev* 1998; 76:91-99.
63. Miller C, Sassoon DA. Wnt-7a maintains appropriate uterine patterning during the development of the mouse female reproductive tract. *Development* 1998; 125:3201-3211.
64. Heikkila M, Peltoketo H, Vainio S. Wnts and the female reproductive system. *J Exp Zool* 2001; 290:616-623.
65. Taylor HS, Vanden Heuvel GB, Igarashi P. A conserved Hox axis in the mouse and human female reproductive system: late establishment and persistent adult expression of the Hoxa cluster genes. *Biol Reprod* 1997; 57:1338-1345.
66. Taylor HS. The role of HOX genes in the development and function of the female reproductive tract. *Semin Reprod Med* 2000; 18:81-89.

67. Mericskay M, Kitajewski J, Sassoon D. Wnt5a is required for proper epithelial-mesenchymal interactions in the uterus. *Development* 2004; 131:2061-2072.
68. Vainio S, Heikkila M, Kispert A, Chin N, McMahon A. Female development in mammals is regulated by Wnt-4 signalling. *Nature* 1999; 397:405-409.
69. Huang WW, Yin Y, Bi Q, Chiang TC, Garner N, Vuoristo J, McLachlan JA, Ma L. Developmental diethylstilbestrol exposure alters genetic pathways of uterine cytodifferentiation. *Mol Endocrinol* 2005; 19:669-682.
70. Tarleton BJ, Wiley AA, Bartol FF. Endometrial development and adenogenesis in the neonatal pig: effects of estradiol valerate and the antiestrogen ICI 182,780. *Biology of Reproduction* 1999; 61:253-263.
71. Hisaw F. Experimental relaxation of the pubic ligament of the guinea pig. *Proceedings of the Society for Experimental Biology and Medicine* 1926; 23:616-623.
72. Bani D. Relaxin: a pleiotropic hormone. *Gen Pharmacol* 1997; 28:13-22.
73. Bathgate RA, Samuel CS, Burazin TC, Gundlach AL, Tregear GW. Relaxin: new peptides, receptors and novel actions. *Trends Endocrinol Metab* 2003; 14:207-213.
74. Hsu SY, Nakabayashi K, Nishi S, Kumagai J, Kudo M, Sherwood OD, Hsueh AJ. Activation of orphan receptors by the hormone relaxin. *Science* 2002; 295:671-674.

75. Parry LJ, McGuane JT, Gehring HM, Kostic IG, Siebel AL. Mechanisms of relaxin action in the reproductive tract: studies in the relaxin-deficient (Rlx^{-/-}) mouse. *Ann N Y Acad Sci* 2005; 1041:91-103.
76. Yao L, Cooke PS, Meling DD, Shanks RD, Jameson JL, Sherwood OD. The effect of relaxin on cell proliferation in mouse cervix requires estrogen receptor {alpha} binding to estrogen response elements in stromal cells. *Endocrinology* 2010; 151:2811-2818.
77. Ferrara N, Gerber HP. The role of vascular endothelial growth factor in angiogenesis. In: *Acta Haematol*, vol. 106. Switzerland: 2001 S. Karger AG, Basel; 2001: 148-156.
78. Gerber HP, Dixit V, Ferrara N. Vascular endothelial growth factor induces expression of the antiapoptotic proteins Bcl-2 and A1 in vascular endothelial cells. *J Biol Chem* 1998; 273:13313-13316.
79. Ziecik AJ. Old, new and the newest concepts of inhibition of luteolysis during early pregnancy in pig. *Domest Anim Endocrinol* 2002; 23:265-275.
80. Cullinan-Bove K, Koos RD. Vascular endothelial growth factor/vascular permeability factor expression in the rat uterus: rapid stimulation by estrogen correlates with estrogen-induced increases in uterine capillary permeability and growth. *Endocrinology* 1993; 133:829-837.
81. Greb RR, Heikinheimo O, Williams RF, Hodgen GD, Goodman AL. Vascular endothelial growth factor in primate endometrium is regulated by oestrogen-receptor and progesterone-receptor ligands in vivo. *Hum Reprod* 1997; 12:1280-1292.

82. Hyder SM, Stancel GM, Chiappetta C, Murthy L, Boettger-Tong HL, Makela S. Uterine expression of vascular endothelial growth factor is increased by estradiol and tamoxifen. *Cancer Res* 1996; 56:3954-3960.
83. Hyder SM, Stancel GM. Regulation of angiogenic growth factors in the female reproductive tract by estrogens and progestins. *Mol Endocrinol* 1999; 13:806-811.
84. Huang JC, Liu DY, Dawood MY. The expression of vascular endothelial growth factor isoforms in cultured human endometrial stromal cells and its regulation by 17beta-oestradiol. *Mol Hum Reprod* 1998; 4:603-607.
85. Marengo SR, Bazer FW, Thatcher WW, Wilcox CJ, Wetteman RP. Prostaglandin F2 alpha as the luteolysin in swine: VI. Hormonal regulation of the movement of exogenous PGF2 alpha from the uterine lumen into the vasculature. *Biol Reprod* 1986; 34:284-292.
86. Ziecik A, Waclawik A, Kaczmarek M, Blitek A, Jalali BM, Andronowska A. Mechanisms for the establishment of pregnancy in the pig. *Reprod Domest Anim* 2011; 46 Suppl 3:31-41.
87. Bazer FW, Thatcher WW. Theory of maternal recognition of pregnancy in swine based on estrogen controlled endocrine versus exocrine secretion of prostaglandin F2alpha by the uterine endometrium. *Prostaglandins* 1977; 14:397-400.
88. Geisert RD, Pratt TN, Bazer FW, Mayes JS, Watson GH. Immunocytochemical localization and changes in endometrial progesterin

- receptor protein during the porcine oestrous cycle and early pregnancy. *Reprod Fertil Dev* 1994; 6:749-760.
89. Spencer TE, Johnson GA, Burghardt RC, Bazer FW. Progesterone and placental hormone actions on the uterus: insights from domestic animals. *Biol Reprod* 2004; 71:2-10.
 90. Bazer FW, Clawson AJ, Robison OW, Ulberg LC. Uterine capacity in gilts. *J Reprod Fertil* 1969; 18:121-124.
 91. Ford S, Vonnahme K, Wilson M. Uterine capacity in the pig reflects a combination of uterine environment and conceptus genotype effects. *Journal of Animal Science (e. Supplement)* 2002; 80:E66–E73.
 92. Biggers JD. Problems concerning the uterine causes of embryonic death, with special reference to the effects of ageing of the uterus. *J Reprod Fertil Suppl* 1969; 8:Suppl 8:27+.
 93. Chen JC, Wiley AA, Ho TY, Frankshun AL, Hord KM, Bartol FF, Bagnell CA. Transient estrogen exposure from birth affects uterine expression of developmental markers in neonatal gilts with lasting consequences in pregnant adults. *Reproduction* 2010; 139:623-630.
 94. Nijland MJ, Ford SP, Nathanielsz PW. Prenatal origins of adult disease. *Curr Opin Obstet Gynecol* 2008; 20:132-138.
 95. Nathanielsz PW. Animal models that elucidate basic principles of the developmental origins of adult diseases. *Ilar J* 2006; 47:73-82.
 96. Fowden AL, Forhead AJ. Hormones as epigenetic signals in developmental programming. *Exp Physiol* 2009; 94:607-625.

97. Holliday R. Epigenetics: a historical overview. *Epigenetics* 2006; 1:76-80.
98. Ho DH, Burggren WW. Epigenetics and transgenerational transfer: a physiological perspective. *J Exp Biol* 2010; 213:3-16.
99. Chmurzynska A. Fetal programming: link between early nutrition, DNA methylation, and complex diseases. *Nutr Rev* 2009; 68:87-98.
100. Nathanielsz PW. Animal models that elucidate basic principles of the developmental origins of adult diseases. *Ilar Journal* 2006; 47:73-82.
101. Bromer JG, Zhou Y, Taylor MB, Doherty L, Taylor HS. Bisphenol-A exposure in utero leads to epigenetic alterations in the developmental programming of uterine estrogen response. *Faseb J* 2010.
102. Samuelsson AM, Matthews PA, Argenton M, Christie MR, McConnell JM, Jansen EH, Piersma AH, Ozanne SE, Twinn DF, Remacle C, Rowlerson A, Poston L, et al. Diet-induced obesity in female mice leads to offspring hyperphagia, adiposity, hypertension, and insulin resistance: a novel murine model of developmental programming. *Hypertension* 2008; 51:383-392.
103. Dong F, Ford SP, Nijland MJ, Nathanielsz PW, Ren J. Influence of maternal undernutrition and overfeeding on cardiac ciliary neurotrophic factor receptor and ventricular size in fetal sheep. *J Nutr Biochem* 2008; 19:409-414.
104. Hinde K, Capitanio JP. Lactational programming? mother's milk energy predicts infant behavior and temperament in rhesus macaques (*Macaca mulatta*). *Am J Primatol* 2010.

105. Burggren W. Genetic, environmental and maternal influences on embryonic cardiac rhythms. *Comparative Biochemistry & Physiology Part A, Molecular & Integrative Physiology* 1999; 124:423-427.
106. Langer P. Differences in the composition of colostrum and milk in eutherians reflect differences in immunoglobulin transfer. *Journal of Mammology* 2009; 90 (2):332-339.
107. Norcross NL. Secretion and composition of colostrum and milk. *J Am Vet Med Assoc* 1982; 181:1057-1060.
108. Jackson KM, Nazar AM. Breastfeeding, the immune response, and long-term health. *Journal of the American Osteopathic Association* 2006; 106:203-207.
109. Fidler N, Koletzko B. The fatty acid composition of human colostrum. *Eur J Nutr* 2000; 39:31-37.
110. Nichols EL, Nichols VN. Human milk: nutritional resource. *Prog Clin Biol Res* 1981; 61:109-146.
111. Grosvenor CE, Picciano MF, Baumrucker CR. Hormones and growth factors in milk. *Endocrine Reviews* 1993; 14:710-728.
112. Buts JP. -Bioactive factors in milk. *Arch Pediatr* 1998; 5:298-306.
113. Farmer C, Houtz SK, Hagen DR. Estrone concentration in sow milk during and after parturition. *J Anim Sci* 1987; 64:1086-1089.
114. Kling PJ. Roles of erythropoietin in human milk. *Acta Paediatrica Supplement* 2002; 91:31-35.

115. Burrin DG, Shulman RJ, Reeds PJ, Davis TA, Gravitt KR. Porcine colostrum and milk stimulate visceral organ and skeletal muscle protein synthesis in neonatal piglets. *J Nutr* 1992; 122:1205-1213.
116. Donovan SM, Odle J. Growth factors in milk as mediators of infant development. *Annu Rev Nutr* 1994; 14:147-167.
117. Kwek JH, Iongh RD, Digby MR, Renfree MB, Nicholas KR, Familiar M. Cross-fostering of the tammar wallaby (*Macropus eugenii*) pouch young accelerates fore-stomach maturation. *Mech Dev* 2009; 126:449-463.
118. Nusser KD, Frawley LS. Is milk a conduit for developmental signals. In: Newburg (ed.) *Bioactive Components of Human Milk*. New York: Kluwer Academic/Plenum Publishers; 2001: 71-77.
119. Ogra SS, Weintraub D, Ogra PL. Immunologic aspects of human colostrum and milk. III. Fate and absorption of cellular and soluble components in the gastrointestinal tract of the newborn. *J Immunol* 1977; 119:245-248.
120. Steinetz BG, Horton L, Lasano S. The source and secretion of immunoactive relaxin in rat milk. *Exp Biol Med (Maywood)* 2009; 234:562-565.
121. Goldsmith LT, Lust G, Steinetz BG. Transmission of relaxin from lactating bitches to their offspring via suckling. *Biology of Reproduction* 1994; 50:258-265.
122. Steinetz BG, Williams AJ, Lust G, Schwabe C, Bullesbach EE, Goldsmith LT. Transmission of relaxin and estrogens to suckling canine pups via milk and possible association with hip joint laxity. *Am J Vet Res* 2008; 69:59-67.

123. Eddie LW, Sutton B, Fitzgerald S, Bell RJ, Johnston PD, Tregear GW. Relaxin in paired samples of serum and milk from women after term and preterm delivery. *American Journal of Obstetrics & Gynecology* 1989; 161:970-973.
124. Frankshun AL, Ho TY, Steinetz BG, Bartol FF, Bagnell CA. Biological activity of relaxin in porcine milk. *Ann N Y Acad Sci* 2009; 1160:164-168.
125. Silva AJ. Defining the Porcine Colostral Proteome: Changes in the Array of Proteins from Colostrum to Mature Milk. 2011. Masters Thesis.
126. Meisel H. Biochemical properties of peptides encrypted in bovine milk proteins. *Curr Med Chem* 2005; 12:1905-1919.
127. Bartol FF, Wiley AA, Bagnell CA. Relaxin and maternal lactocrine programming of neonatal uterine development. *Ann N Y Acad Sci* 2009; 1160:158-163.
128. Chen JC, A F, Wiley AA, Welch KA, Ho TY, Bartol FF, Bagnell CA. Milk-borne lactocrine-acting factors affect gene expression patterns in the developing neonatal porcine uterus. *Reproduction* 2011; 141 (In Press; DOI: 10.1530/REP-10-0320).
129. Chen J. Factors that define the developmental program and trajectory of the porcine uterus. Rutgers University; 2010. PhD Dissertation.
130. Frankshun A. The role of nursing on maternal programming of the neonatal porcine cervix. Rutgers University; 2011.
131. Eltoun IA, Siegal GP, Frost AR. Microdissection of histologic sections: past, present, and future. *Adv Anat Pathol* 2002; 9:316-322.

132. Hernandez S, Lloreta J. Manual versus laser micro-dissection in molecular biology. In: *Ultrastruct Pathol*, vol. 30. United States; 2006: 221-228.
133. Espina V, Wulfschlegel JD, Calvert VS, VanMeter A, Zhou W, Coukos G, Geho DH, Petricoin EF, 3rd, Liotta LA. Laser-capture microdissection. In: *Nat Protoc*, vol. 1. England; 2006: 586-603.
134. Espina V, Heiby M, Pierobon M, Liotta LA. Laser capture microdissection technology. *Expert Rev Mol Diagn* 2007; 7:647-657.
135. Thornhill DJ, Fielman KT, Santos SR, Halanych KM. *Siboglinid-bacteria endosymbiosis: A model system for studying symbiotic mechanisms.* *Commun Integr Biol* 2008; 1:163-166.
136. Hartmann S, Bergmann M, Bohle RM, Weidner W, Steger K. Genetic imprinting during impaired spermatogenesis. In: *Mol Hum Reprod*, vol. 12. England; 2006: 407-411.
137. Wulfschlegel JD, Sgroi DC, Krutzsch H, McLean K, McGarvey K, Knowlton M, Chen S, Shu H, Sahin A, Kurek R, Wallwiener D, Merino MJ, et al. Proteomics of human breast ductal carcinoma in situ. *Cancer Res* 2002; 62:6740-6749.
138. Jones MB, Krutzsch H, Shu H, Zhao Y, Liotta LA, Kohn EC, Petricoin EF, 3rd. Proteomic analysis and identification of new biomarkers and therapeutic targets for invasive ovarian cancer. In: *Proteomics*, vol. 2. Germany; 2002: 76-84.
139. Ornstein DK, Englert C, Gillespie JW, Pawletz CP, Linehan WM, Emmert-Buck MR, Petricoin EF, 3rd. Characterization of intracellular prostate-specific

- antigen from laser capture microdissected benign and malignant prostatic epithelium. *Clin Cancer Res* 2000; 6:353-356.
140. Umar A, Kang H, Timmermans AM, Look MP, Meijer-van Gelder ME, den Bakker MA, Jaitly N, Martens JW, Luider TM, Foekens JA, Pasa-Tolic L. Identification of a putative protein profile associated with tamoxifen therapy resistance in breast cancer. In: *Mol Cell Proteomics*, vol. 8. United States; 2009: 1278-1294.
141. Paweletz CP, Liotta LA, Petricoin EF, 3rd. New technologies for biomarker analysis of prostate cancer progression: Laser capture microdissection and tissue proteomics. In: *Urology*, vol. 57. United States; 2001: 160-163.
142. Buckanovich RJ, Sasaroli D, O'Brien-Jenkins A, Botbyl J, Hammond R, Katsaros D, Sandaltzopoulos R, Liotta LA, Gimotty PA, Coukos G. Tumor vascular proteins as biomarkers in ovarian cancer. *J Clin Oncol* 2007; 25:852-861.
143. Gjerdrum LM, Abrahamsen HN, Villegas B, Sorensen BS, Schmidt H, Hamilton-Dutoit SJ. The influence of immunohistochemistry on mRNA recovery from microdissected frozen and formalin-fixed, paraffin-embedded sections. *Diagn Mol Pathol* 2004; 13:224-233.
144. Gjerdrum LM, Hamilton-Dutoit S. Laser-assisted microdissection of membrane-mounted sections following immunohistochemistry and in situ hybridization. *Methods Mol Biol* 2005; 293:139-149.
145. Wiley AA, Kauffold J, Waehner M, Crean-Harris BD, Miller DJ, Bagnell CA, Bartol FF. Laser microdissection of neonatal porcine endometrium for tissue

- specific evaluation of relaxin receptor (RXFP1) expression in response to perinatal zearalenone exposure. *Annals of the New York Academy of Sciences* 2008.
146. Chan S, Murray PG, Franklyn JA, McCabe CJ, Kilby MD. The use of laser capture microdissection (LCM) and quantitative polymerase chain reaction to define thyroid hormone receptor expression in human 'term' placenta. In: *Placenta*, vol. 25. England; 2004: 758-762.
 147. Tsubota K, Kanki M, Noto T, Shiraki K, Takeuchi A, Nakatsuji S, Seki J, Oishi Y, Matsumoto M, Nakayama H. Transitional Gene Expression Profiling in Ovarian Follicle during Ovulation in Normal-Cycle Rats. *Toxicol Pathol* 2011; 39:641-652.
 148. Li J, Todd TC, Lee J, Trick HN. Biotechnological application of functional genomics towards plant-parasitic nematode control. *Plant Biotechnol J* 2011.
 149. Nelson T, Tausta SL, Gandotra N, Liu T. Laser microdissection of plant tissue: what you see is what you get. *Annu Rev Plant Biol* 2006; 57:181-201.
 150. Vandewoestyne M, Deforce D. Laser capture microdissection in forensic research: a review. *Int J Legal Med* 2010; 124:513-521.
 151. Chimenti C, Pieroni M, Russo A, Sale P, Russo MA, Maseri A, Frustaci A. Laser microdissection in clinical cardiovascular research. *Chest* 2005; 128:2876-2881.
 152. Hunt JL, Finkelstein SD. Microdissection techniques for molecular testing in surgical pathology. *Arch Pathol Lab Med* 2004; 128:1372-1378.

153. Okuducu AF, Hahne JC, Von Deimling A, Wernert N. Laser-assisted microdissection, techniques and applications in pathology (review). *Int J Mol Med* 2005; 15:763-769.
154. Standaert DG. Applications of laser capture microdissection in the study of neurodegenerative disease. *Arch Neurol* 2005; 62:203-205.
155. Kondo T. Tissue proteomics for cancer biomarker development: laser microdissection and 2D-DIGE. *BMB Rep* 2008; 41:626-634.
156. Viñas J, Piferrer F. Stage-Specific Gene Expression During Fish Spermatogenesis as Determined by Laser-Capture Microdissection and Quantitative-PCR in Sea Bass (*Dicentrarchus labrax*) Gonads. *BIOLOGY OF REPRODUCTION* 2008; 79:738-747.
157. Chinge NO, Ruddle F, Bayarsaihan D. Laser-assisted microdissection (LAM) in developmental biology. *J Exp Zool B Mol Dev Evol* 2007; 308:113-118.
158. Pinzani P, Orlando C, Pazzagli M. Laser-assisted microdissection for real-time PCR sample preparation. *Mol Aspects Med* 2006; 27:140-159.
159. Srinivasan M, Sedmak D, Jewell S. Effect of fixatives and tissue processing on the content and integrity of nucleic acids. *Am J Pathol* 2002; 161:1961-1971.
160. Gugic D, Nassiri M, Nadji M, Morales A, Vincek V. Novel tissue preservative and tissue fixative for comparative pathology and animal research. *Journal of Experimental Animal Science* 2007; 43:271-281.
161. Cox ML, Schray CL, Luster CN, Stewart ZS, Korytko PJ, Khan KNM, Paulauskis JD, Dunstan RW. Assessment of fixatives, fixation, and tissue

- processing on morphology and RNA integrity. *Experimental and Molecular Pathology* 2006; 80:183-191.
162. von Ahlfen S, Missel A, Bendrat K, Schlumpberger M. Determinants of RNA quality from FFPE samples. *PLoS One* 2007; 2:e1261.
163. Stanta G, Bonin S, Perin R. RNA extraction from formalin-fixed and paraffin-embedded tissues. *Methods Mol Biol* 1998; 86:23-26.
164. Ambion. Precipitation of nucleic acids;
www.ambion.com/techlib/helpdesk/index.htm/. 2011.
165. Fisher Scientific BioAssays;
www.fishersci.com/ecom/servlet/cmstatic/productservices/chemicals. 2011.
166. Qiagen. Assay Technologies;
www.qiagen.com/me/ffpepurification/default/rnaisolation+from+tissue.
2011.
167. Bustin SA, Benes V, Nolan T, Pfaffl MW. Quantitative real-time RT-PCR--a perspective. *J Mol Endocrinol* 2005; 34:597-601.
168. Dieffenbach CW, Lowe TM, Dveksler GS. General concepts for PCR primer design. *PCR Methods Appl* 1993; 3:S30-37.
169. Antonov J, Goldstein DR, Oberli A, Baltzer A, Pirotta M, Fleischmann A, Altermatt HJ, Jaggi R. Reliable gene expression measurements from degraded RNA by quantitative real-time PCR depend on short amplicons and a proper normalization. *Lab Invest* 2005; 85:1040-1050.
170. Abd-Elsalam KA. Bioinformatic tools and guidelines for PCR primer design. *African Journal of Biotechnology* 2003; 2:91-95.

171. Cox ML, Eddy SM, Stewart ZS, Kennel MR, Man MZ, Paulauskis JD, Dunstan RW. Investigating fixative-induced changes in RNA quality and utility by microarray analysis. In: *Exp Mol Pathol*, vol. 84. United States; 2008: 156-172.
172. Vincek V, Nassiri M, Nadji M, Morales AR. A tissue fixative that protects macromolecules (DNA, RNA, and protein) and histomorphology in clinical samples. *Lab Invest* 2003; 83:1427-1435.
173. Gray CA, Taylor KM, Ramsey WS, Hill JR, Bazer FW, Bartol FF, Spencer TE. Endometrial glands are required for preimplantation conceptus elongation and survival. *Biology of Reproduction* 2001; 64:1608-1613.
174. Bustin SA, Benes V, Garson JA, Hellemans J, Huggett J, Kubista M, Mueller R, Nolan T, Pfaffl MW, Shipley GL, Vandesompele J, Wittwer CT, et al. The MIQE guidelines: minimum information for publication of quantitative real-time PCR experiments. *Clinical Chemistry* 2009; 55:611-622.
175. Hondares E, Rosell M, Gonzalez FJ, Giralt M, Iglesias R, Villarroya F. Hepatic FGF21 expression is induced at birth via PPARalpha in response to milk intake and contributes to thermogenic activation of neonatal brown fat. *Cell Metabolism* 2010; 11:206-212.
176. Lefevre CM, Sharp JA, Nicholas KR. Evolution of lactation: ancient origin and extreme adaptations of the lactation system. *Annu Rev Genomics Hum Genet* 2010; 11:219-238.

177. Peaker M. The mammary gland in mammalian evolution: a brief commentary on some of the concepts. *Journal of Mammary Gland Biology & Neoplasia* 2002; 7:347-353.
178. Barker D. *Mothers, Babies and Health in Later Life*. Edinburgh: Churchill Livingstone; 1998.
179. Mousseau TA, Fox CW. *Maternal Effects as Adaptations*. New York: Oxford University Press; 1998.
180. Jirtle RL, Skinner MK. Environmental epigenomics and disease susceptibility. *Nature Reviews Genetics* 2007; 8:253-262.
181. Bartol FF, Bagnell CA. Lactocrine programming of female reproductive tract development: environmental connections to the reproductive continuum. *Mol Cell Endocrinol* 2012; 354:16-21.
182. Bartol FF, Wiley AA, Miller DJ, Silva AJ, Roberts KE, Davolt ML, Chen JC, Frankshun AL, Camp ME, Rahman KM, Vallet JL, Bagnell CA. Lactocrine signaling and developmental programming. *J Anim Sci* 2012.
183. Oftedal OT. The mammary gland and its origin during synapsid evolution. *J Mammary Gland Biol Neoplasia* 2002; 7:225-252.
184. Neville MC, Anderson SM, McManaman JL, Badger TM, Bunik M, Contractor N, Crume T, Dabelea D, Donovan SM, Forman N, Frank DN, Friedman JE, et al. Lactation and neonatal nutrition: defining and refining the critical questions. *J Mammary Gland Biol Neoplasia* 2012; 17:167-188.

185. Joss JL, Molloy MP, Hinds L, Deane E. A longitudinal study of the protein components of marsupial milk from birth to weaning in the tammar wallaby (*Macropus eugenii*). *Dev Comp Immunol* 2009; 33:152-161.
186. Trott JF, Simpson KJ, Moyle RL, Hearn CM, Shaw G, Nicholas KR, Renfree MB. Maternal regulation of milk composition, milk production, and pouch young development during lactation in the tammar wallaby (*Macropus eugenii*). *Biology of Reproduction* 2003; 68:929-936.
187. Grosvenor CE, Mena F. Regulation of prolactin transformation in the rat pituitary. *Ciba Found Symp* 1992; 168:69-80; discussion 80-66.
188. Almeida AA, Lopes CM, Silva AM, Barrado E. Trace elements in human milk: correlation with blood levels, inter-element correlations and changes in concentration during the first month of lactation. *J Trace Elem Med Biol* 2008; 22:196-205.
189. Lemay DG, Lynn DJ, Martin WF, Neville MC, Casey TM, Rincon G, Kriventseva EV, Barris WC, Hinrichs AS, Molenaar AJ, Pollard KS, Maqbool NJ, et al. The bovine lactation genome: insights into the evolution of mammalian milk. *Genome Biol* 2009; 10:R43.
190. Simmen FA, Cera KR, Mahan DC. Stimulation by colostrum or mature milk of gastrointestinal tissue development in newborn pigs. *J Anim Sci* 1990; 68:3596-3603.
191. Shulman RJ. Oral insulin increases small intestinal mass and disaccharidase activity in the newborn miniature pig. *Pediatr Res* 1990; 28:171-175.

192. Field CJ. The immunological components of human milk and their effect on immune development in infants. *J Nutr* 2005; 135:1-4.
193. Kosaka N, Izumi H, Sekine K, Ochiya T. microRNA as a new immune-regulatory agent in breast milk. *Silence* 2010; 1:7.
194. Lonnerdal B. Nutritional and physiologic significance of human milk proteins. *Am J Clin Nutr* 2003; 77:1537S-1543S.
195. Calder PC, Krauss-Etschmann S, de Jong EC, Dupont C, Frick JS, Frokiaer H, Heinrich J, Garn H, Koletzko S, Lack G, Mattelio G, Renz H, et al. Early nutrition and immunity - progress and perspectives. *British Journal of Nutrition* 2006; 96:774-790.
196. Frankshun AL, Chen J, Barron LA, Ho TY, Miller DJ, Rahman KM, Bartol FF, Bagnell CA. Nursing during the first two days of life is essential for the expression of proteins important for growth and remodeling of the neonatal porcine cervix. *Endocrinology* 2012; 153:4511-4521.
197. Chen JC, Frankshun AL, Wiley AA, Miller DJ, Welch KA, Ho TY, Bartol F, Bagnell C. Milk-borne lactocrine-acting factors affect gene expression patterns in the developing neonatal porcine uterus. *Reproduction* 2011.
198. Bigsby RM, Cunha GR. Effects of progestins and glucocorticoids on deoxyribonucleic acid synthesis in the uterus of the neonatal mouse. *Endocrinology* 1985; 117:2520-2526.
199. Ogasawara Y, Okamoto S, Kitamura Y, Matsumoto K. Proliferative pattern of uterine cells from birth to adulthood in intact, neonatally castrated, and/or

- adrenalectomized mice, assayed by incorporation of [125I]iododeoxyuridine. *Endocrinology* 1983; 113:582-587.
200. Iatropoulos MJ, Williams GM. Proliferation markers. *Exp Toxicol Pathol* 1996; 48:175-181.
201. Pillai SB, Rockwell LC, Sherwood OD, Koos RD. Relaxin stimulates uterine edema via activation of estrogen receptors: blockade of its effects using ICI 162,780, a specific estrogen receptor antagonist. *Endocrinology* 1999; 140:2426-2429.
202. Lubahn DB, Moyer JS, Golding TS, Couse JF, Korach KS, Smithies O. Alteration of reproductive function but not prenatal sexual development after insertional disruption of the mouse estrogen receptor gene. *Proc Natl Acad Sci U S A* 1993; 90:11162-11166.
203. Park S, Yoon S, Zhao Y, Park SE, Liao L, Xu J, Lydon JP, DeMayo FJ, O'Malley BW, Bagchi MK, Katzenellenbogen BS. Uterine development and fertility are dependent on gene dosage of the nuclear receptor coregulator REA. *Endocrinology* 2012; 153:3982-3994.
204. Bazer FW. Fertility: role of repressor of estrogen receptor activity. *Endocrinology* 2012; 153:3555-3557.
205. Bigsby RM, Li AX, Luo K, Cunha GR. Strain differences in the ontogeny of estrogen receptors in murine uterine epithelium. *Endocrinology* 1990; 126:2592-2596.

206. Cunha GR, Young P, Brody JR. Role of uterine epithelium in the development of myometrial smooth muscle cells. *Biol Reprod* 1989; 40:861-871.
207. Cunha GR, Chung LW, Shannon JM, Taguchi O, Fujii H. Hormone-induced morphogenesis and growth: role of mesenchymal-epithelial interactions. *Recent Prog Horm Res* 1983; 39:559-598.
208. Reardon SN, King ML, MacLean JA, 2nd, Mann JL, DeMayo FJ, Lydon JP, Hayashi K. CDH1 is essential for endometrial differentiation, gland development, and adult function in the mouse uterus. *Biol Reprod* 2012; 86:141, 141-110.
209. Yin Y, Huang WW, Lin C, Chen H, MacKenzie A, Ma L. Estrogen suppresses uterine epithelial apoptosis by inducing *birc1* expression. *Mol Endocrinol* 2008; 22:113-125.
210. Vallet JL, Miles JR, Rempel LA. A simple novel measure of passive transfer of maternal immunoglobulin is predictive of preweaning mortality in piglets. *Vet J* 2013; 195: 91-97.

Appendix A.

Laser Microdissection Slide Preparation

Materials:

1. Tissues fixed in Xpress Molecular Fixative and embedded in Paraplast Plus.
2. MMI MembraneSlides (Molecular Machines and Industries)
3. Hemo-De,
4. 100% ETOH and 70% ETOH
5. RNase-free H₂O
6. MMI Staining Kit (Molecular Machines and Industries)

all procedures are performed in an RNase-free environment

Procedure:

1. Section tissues at 10 µm thick. Mount sections on MMI MembraneSlides. For isolation of whole endometrium 10-12 sections are needed. For isolation of epithelium and stroma 20-22 sections are needed.
2. Allow slides to dry at 42°C for 45-60 minutes.
3. To deparaffinize and stain slides:
 - a) Prepare 2 containers of Hemo-De, 2 containers of 100% ETOH, 2 containers of 70% ETOH, and 1 container of RNase-free H₂O.
 - b) Place slides into Hemo-De for 4 minutes.
 - c) Move slides to second Hemo-De for 3 minutes. Dunk slides several times to best remove Paraplast.
 - d) Move slides to first 100% ETOH for 4 minutes. Dunk slides.
 - e) Move slides to first 70% ETOH for 1-2 minutes.

- d) Rinse slides in RNase-free H₂O (X2) until free of Hemo-DE and ETOH.
- f) Remove slides from H₂O and shake to remove excess.
- g) Stain slides with MMI Staining Kit Solution 3 (hematoxylyn) for 2 minutes.
Shake slides to remove excess stain.
- h) Add MMI Staining Kit Solution 2 to slides for 30 seconds. Shake to remove excess.
- i) Place slide in second 70% ETOH for 30-60 seconds until stain begins to clear.
- k) Move slides to second 100% ETOH for 30 seconds.
- l) Remove slides from solution and allow to air dry. (~10 minutes)

Appendix B.

Laser Microdissection Process

Materials:

1. LMD Workstation and software
2. MMI MembraneSlide (Molecular Machines and Industries) with tissue sections
3. Glass slides
4. MMI IsolationCaps (Molecular Machines and Industries)
5. Ice

*** all procedures are performed in a RNase-free environment***

Procedures:

MMI Workstation Start-Up:

1. Turning on the Machine
 - a) Turn on the computer tower first, followed by the computer screen and lamp. Allow the computer to fully boot up.
 - b) First, turn the key then press the button on the blue laser/camera power box. An orange and green light will appear.
2. Starting up the MMI Software
 - a) Double click the MMI icon on the desktop.
 - b) Once the program is open check to make sure the program is recognizing the laser and camera. This can be found in the top left hand corner of the screen. If the program is running correctly there will be a green dot followed by the words 'hardware is OK'. If there is an error message, close the program and restart the computer following the above instructions again.

3. Preparing the Sample

- a. Place the MMI membrane slide on a regular glass slide with trough side up (tissue side down). Place and secure both slides on the stage.
- b) Place a MMI IsolationCap Tube in the cap holder.

4. Mapping the Slide

- a) Set the microscope and software objective to 4X.
- b) Find the top left corner of your slide in on the screen. Click the 'set limit button' in the toolbar at the top of the screen. Now find the bottom right corner of the slide and set the lower limit button. To map slide click the button in the right panel with a winding arrow.

5. Calibrating the Laser

- a) Set the microscope and software to 20x. Move the field of view to an empty area.
- b) The green target in the center of the screen is where the laser fires. Fire the laser 2-3 times by clicking the laser button in the right panel. Locate the spot where the laser fired.
- c) Under the UVCut tab > Laser > Set laser position. This will change the green target to a white target controlled by the mouse. Center the white target over where the laser fired and right click. Laser is calibrated.

6. Calibrating the Objectives

- a) Set the microscope and the software to the objective you plan to use. Move the field of view to an area with a memorable area/spot.
- b) Under the UVCut Tab > Objective > Calibration

- c) A menu box will appear on the screen. Click 'Calibrate' in the box. The mouse will turn into a white target and two boxes will appear in the top left and bottom right of the field of view.
- d) Locate the unique area on the slide. Hit the space bar to use the grab tool to move the field of view. Move the chosen area into the center of the top left box. Hit the space bar again to return to the target tool. Place the target in the center of the same box and click.
- e) Hit space bar again to return to the grab tool and move the area of choice into the bottom right box. Hit space bar again to return to target tool. Click in the center of the box.
- f) Right click in the center of the screen. The menu box will return. Click ok.

Appendix C.

LMD of Uterine Tissues:

1. Identify the region of interest (ROI): endometrium, epithelium, stroma, myometrium, etc.
2. Excising the ROI
 - a) To draw click the pen button in the right panel. Use the stylus to draw around the ROI you wish to excise. You may draw as many areas as necessary.
 - b) When finished drawing lower the cap using the arrow button in the right panel.
 - c) Click the cut button to fire the laser and excise the region of interest.
 - d) When laser finishes raise the cap using the arrow button. The ROI is now isolated on the MMI IsolationCap. Repeat this process as many times as necessary.
 - e) Change cap when it becomes covered in tissues and when isolating different ROIs.
 - f) Place tubes with tissue on ice when finished.

Appendix D.

RNA Extraction

Materials:

1. RecoverAll Total Nucleic Acid Isolation Kit (Ambion)
2. Excised samples
3. 100% ETOH
4. RNase Inhibitor (Ambion)
5. Appropriate size microfuge tubes (size depends on # of samples)
6. RNase-free H₂O

*** all procedures are performed in a RNase-free environment***

Procedure: (as adapted from RecoverAll manufacturer's instructions)

(Day 1)

1. Add 200 µl Digestion Buffer to each sample.
2. Add 4 µl Protease to each sample.
3. Vortex samples gently to mix.
4. Incubate samples *upside down*, overnight (14-16 hours) at 50° C.

(Day 2)

5. Incubate samples upside down for 15 minutes at 80° C.
6. Prepare Isolation Mixture: *mixture should be made using estimated 5% overage*
 - a) In an appropriate size microfuge tube, add 200 µl Isolation Additive/sample.
 - b) Add 550 µl 100% ETOH/sample. Vortex gently to mix.

7. Add 790 μ l Isolation Mixture to each sample. Pipet up and down to mix.
8. For each sample place Filter Cartridge into supplied Collection Tubes.
9. Pipet 700 μ l of sample/Isolation mixture onto Filter Cartridge and close the lid.
10. Centrifuge at 10,000 rpm for 30 seconds.
11. Discard flow-through and re-place Filter Cartridge in same Collection Tube.
12. Repeat steps 9-11 until all sample/Isolation Mixture has passed through the filter.
13. Add 700 μ l of Wash 1 to the Filter Cartridge.
14. Centrifuge at 10,000 rpm for 30 seconds.
15. Discard flow-through and re-place Filter Cartridge into the same Collection Tube.
16. Add 500 μ l of Wash 2/3 to the Filter Cartridge.
17. Centrifuge at 10,000 rpm for 30 seconds.
18. Discard flow-through and re-place Filter Cartridge into the same Collection Tube.
19. Centrifuge the assembly at 10,000 rpm for an additional 30 seconds to remove excess fluid from the filter.
20. Nuclease Digestion:
 - a) Prepare DNase Mixture: In a new microfuge tube combine:
 - i) 6 μ l 10X DNase Buffer/sample
 - ii) 4 μ l DNase/sample
 - iii) 50 μ l RNase-free H₂O/sample
 - b) Add 60 μ l of DNase Mixture to the center of each Filter Cartridge.

- c) Close the cap of the Collection Tube and incubate at room temperature for 30 minutes.
21. Add 700 μ l of Wash 1 to the Filter Cartridge.
 22. Incubate for 1 min at room temperature.
 23. Centrifuge at 10,000 rpm for 30 seconds.
 24. Discard flow-through and re-place Filter Cartridge into the same Collection Tube.
 25. Add 500 μ l of Wash 2/3 to the Filter Cartridge.
 26. Centrifuge at 10,000 rpm for 30 seconds
 27. Discard flow-through and re-place Filter Cartridge into the same Collection Tube.
 28. Repeat steps 25-27.
 29. Centrifuge assembly at 10,000 rpm for 1 minute.
 30. Transfer Filter Cartridge to NEW Collection tube.
 31. Add 60 μ l of room temperature RNase-free H₂O to the center of the filter and close the cap.
 32. Incubate at room temperature for 1-2 minutes.
 33. Centrifuge at 16,000 rpm for 2 minutes. This eluate contains RNA.
 34. Add 0.5 μ l of RNase Inhibitor to each sample.
 35. Speed-vac samples for 30 minutes or until desired concentration is reached.
 36. Store at -20° C.

Appendix E.

Quantitative Real Time PCR (qPCR)

Materials:

1. High Capacity cDNA Reverse Transcription Kit (Applied Biosystems)
2. RNA samples
3. RNase Inhibitor (Ambion)
4. Power SYBR Green PCR Master Mix (Applied Biosystems)
5. Both forward and reverse primer for target gene
6. cDNA diluted to 10 ng/ μ l
7. MicroAmp 8 ct. Optical Tube and Cap Strips (Applied Biosystems)
8. RNase-free H₂O

all procedures performed in a nuclease-free environment and on ice

Procedure:

1. Generate cDNA:
 - a) Convert 500 ng of total RNA to 500 ng of cDNA using the High Capacity Reverse Transcriptase Kit. This may not work for all samples. Do so following the manufacturer's instructions using the 50 μ l reaction volume.
2. Reconstitute lyophilized primers to 1mM with 1x TE.
3. Dilute reconstituted primers to 2 μ M in volume needed (usually around 500 μ l).
4. Create a standard curve using generated cDNA from same tissue type as samples. For LMD, curves generally consisted of 40x, 20x, 10x, 5x, and 2.5x. (10x = 10 ng)
Also needed is a negative control or no template control (NTC). There should be a standard curve and NTC for each gene used.

5. For qPCR the 25 μ l reaction volume was used is duplicate with 10 μ l being sample and 15 μ l of master mix. Make enough master mix for standard curve + # of samples + NTC in each run. This must be done separately for each gene. Remember this is done in duplicate so the final total of reactions should be multiplied by 2. Add 4-5 extra reactions to account for pipetting error.
6. Master mix is prepared in dim light and separate tubes for each gene. For master mix: per reaction add 12.5 μ l SYBR Green, add 1.25 μ l of forward primer, and add 1.25 μ l of reverse primer (refer to SYBR Green manufacturer's instructions). Final primer concentration should be 100 nM for forward and reverse primers. This may need to be optimized (see ABI User Bulletin #2 for Primer Validation and SYBR Green PCR Master Mix protocol).
7. Mix the master mix by pipetting up and down or by *vortexing gently*. Quick-spin to remove bubbles.
8. Prepare samples in separate 0.5 ml tubes. For LMD, reactions contained 5 ng of sample. Total sample volume = 21 μ l. Nuclease-free H₂O is used to bring the sample up to volume.
9. Add 32 μ l of master mix to each sample tube. (29 μ l master mix x 0.1% error = 32 μ l) This makes the total volume 53 μ l of sample + master mix. Mix by pipetting up and down. Quick-spin to remove bubbles.
10. Aliquot 25 μ l of each reaction mixture into separate optical tubes.
11. Cap the tubes. Label strips on the top tab NOT on the optical caps. This will interfere with the reaction. Quick-spin to remove bubbles.

12. Use the Applied Biosystems 7500 Real Time PCR system to run the assay. Refer to the manufacturer's instructions to run the assay.

Appendix F.

Immunohistochemistry

Materials:

1. ESR1: DAKO mouse monoclonal 1D5; 1:100
2. PCNA: Zymed/Invitrogen mouse monoclonal 1:500.
3. VECTASTAIN ABC Elite Kit (Goat) (Vector Labs)
4. Goat IgG
5. 1x PBS
6. Hemo-De
7. 100% ETOH, 95% ETOH, and 70% ETOH
8. 3% Hydrogen peroxide
9. Citric Acid-mono hydrate
10. Sodium Citrate dihydrate
11. DAB
12. BSA

Procedure:

1. Section tissues at 6 μ m thick.
2. Mount 2 non-sequential sections per animal on frosted glass slides.
3. Allow slides to dry overnight.
4. To deparaffinize slides:
 - a) Prepare 2 containers Hemo-De, 2 containers 100% ETOH, 2 containers 95% ETOH, 1 container 70% ETOH, and 1 container H₂O.
 - b) Submerge slides for 3 minutes in each container sequentially.

5. Boil in 600 ml of 10mM Citrate buffer pH 6.0 for 15 minutes.
6. Cool in Citrate buffer for 15 minutes.
7. Wash in PBS 3x for 3 minutes each.
8. Circle individual section with immuopen.
9. Block with normal serum for 20 minutes. Follow ABC Elite Kit manufacturer's instructions.
10. Apply primary anti-body for ESR1 (mouse monoclonal anti-ESR1 (DAKO; 1D5,1:100) or for PNCA (mouse monoclonal anti-PCNA (Zymed/Invitrogen, 1:500). Negative control sections were incubated with mouse isotype control IgG (Zymed/Invitrogen). Incubate overnight at 4° C.
11. Wash slides in PBS 3 minutes.
12. Apply secondary antibody following ABC Elite Kit instructions. Incubate for 10 minutes.
13. Wash in PBS for 3 minutes.
14. Place slides in 3% hydrogen peroxide for 5 minutes.
15. Rinse in H₂O then wash in PBS for 3 minutes.
16. Apply ABC reagent and incubate at room temperature for 30 minutes.
17. Wash slides in PBS for 3 minutes.

18. Develop slides in 0.01% DAB in 0.1M Tris (pH 7.5) and 0.2% hydrogen peroxide in H₂O.